NASA Contractor Report 181870

Monolithic Narrow-Linewidth InGaAsP Semiconductor Laser for Coherent Optical Communications

S. L. Palfrey
R. E. Enstrom
P. A. Longeway

David Sarnoff Research Center
Princeton, NJ 08543-5300

Contract NAS1-18539

September 1989

Final Report

for the period 6 August 1987 to 9 June 1989

National Aeronautics and
Space Administration

Langley Research Center
Hampton, Virginia 23665-5225

PREFACE

This Final Report covers work performed at the David Sarnoff Research Center (Sarnoff) from August 6, 1987 to June 9, 1989, under Contract No. NAS1-18539, by the Optoelectronics Research Laboratory, M. Ettenberg, Director. The Program Manager was R. A. Bartolini, Head, Laser Diode Systems, and the Project Scientist was S. L. Palfrey. Personnel who contributed to this work, in addition to those mentioned above, are listed below.

	J. T. Andrews	Fabrication
	J. R. Appert	MOCVD Growth
*	D. J. Channin	Design
	N. DiGiuseppe	Fabrication
*	R. E. Enstrom	MOCVD Growth
*	G. A. Evans	Design
	D. B. Gilbert	Characterization
	M. G. Harvey	Mounting
	F. Z. Hawrylo	Growth and Fabrication
	J. Jaklik, Jr.	VPE Growth
	J. B. Kirk	Grating Fabrication
*	P. A. Longeway	VPE Growth
	E. A. Miller	VPE Growth
	R. Stolzenberger	Characterization
	D. T. Tarangioli	Fabrication
	A. R. Triano, Jr.	Fabrication

* Member of Technical Staff

SUMMARY

This report reviews work carried out at the David Sarnoff Research Center (Sarnoff) during the first year of a four-year research program to develop monolithically integrated, narrow-spectral-linewidth InGaAsP semiconductor lasers. The specific objective of this program was to develop a device that would fulfill the requirements for a large variety of coherent lightwave communication systems, such as high-bit-rate, single-channel systems and multi-channel, wavelength-division-multiplexed systems. In addition, the integrated optics technology developed under this program would be directly applicable to the development of other integrated optical devices and circuits.

The major effort during Phase 1 of this program was to develop a design for a monolithic, narrow-linewidth device and then develop the semiconductor growth and fabrication techniques required to realize this structure. Based on an analysis of a number of designs, including both distributed feedback (DFB) and distributed-Bragg-reflector (DBR) lasers, we have developed a design based on an InGaAs multiple-quantum-well (MQW) DBR laser with an integrated passive waveguide and MQW modulator.

This design incorporates a number of features at the leading edge of semiconductor laser technology that require further development. In particular, this structure requires the integration of the active elements, for the gain and modulator sections, with low-loss passive waveguides. Since these disparate elements have very different requirements on the semiconductor material, new integration techniques had to be developed. This narrow-linewidth laser design also proposed to use InGaAs MQW laser structures, which are at the leading edge of semiconductor laser technology.

During the first year, we have developed, using a non-quantum-well structure, many of the fabrication techniques required for the integration of the narrow-linewidth device. Based on this effort, we have now demonstrated a DBR laser structure that is compatible with our ultimate MQW design and can serve as the building block for this device.

In parallel with the development of the fabrication, we have developed the MOCVD growth of MQW laser structures in the InGaAsP material system. We have now demonstrated room-temperature operation of InGaAs/InGaAsP MQW

lasers with threshold current densities that are comparable to the best reported in the literature.

At this point, we are in a position to incorporate the MQW laser structures into the DBR laser structure developed during Phase 1. The incorporation of the MQW structure into the DBR cavity will also automatically allow for the monolithic integration of modulators. Therefore, all the elements required for the proposed narrow-linewidth laser structure are in place.

Table of Contents

List of Illustrations

List of Illustrations
(cont'd.)

List of Illustrations
(cont'd.)

List of Illustrations
(cont'd.)

Section I

INTRODUCTION

'his report reviews work carried out at the David Sarnoff Research Center f) during the first year of a four-year research program to develop hically integrated, narrow-spectral-linewidth semiconductor lasers. The objective of this four-year program is to develop a device that is fully table into a communications system. Furthermore, these sources should he requirements for a large variety of coherent lightwave communication s such as high-bit-rate, single-channel systems and multi-channel, ngth-division-multiplexed systems. The integrated optics technology we eloping for these will also be directly applicable to the development of other ted optical devices and circuits.

oherent optical communications systems require laser sources and local ors that have a spectral linewidth significantly less than the data dth. As shown in Fig. 1, amplitude-shift keying and frequency-shift require that the transmitter and local oscillator linewidth be about 9% of rate, while for homodyne phase-shift keying, which is potentially the sensitivity format, the linewidth requirement is much more severe at f the bit rate.[1] The linewidth requirements of the system, therefore, vary . However, it is clear that linewidths much less than 1 MHz is desirable y applications. Even at bit rates as high as 1 Gbit/s, linewidths on the 100 kHz are required for homodyne phase-shift keying. Furthermore, for rate, wavelength-division multiplexed systems that might carry only /s per channel, a linewidth of less than 1 MHz is required even for ASK , and a PSK format would require a linewidth on the order of 10 kHz.

ased on the range of requirements for coherent communications systems, een the objective of this research effort to demonstrate an integratable hic narrow linewidth semiconductor laser with the following operational ristics: (1) cw power output in the 1- to 10-mW range, (2) single spatial put with diffraction-limited beam, (3) modulation capability (either direct separate integrated modulators) in the 0.3- to- 4-GHz range, (4) laser linewidth in the 10- to 100-kHz range with a side mode rejection ratio in e of from 20 to 50 dB, (5) laser center wavelength stability better than 10 to

100 kHz, and (6) demonstration of all operational characteristics simultaneously. Many of these characteristics, such as linewidths in the range of 10 to 100 kHz, have been achieved in hybrid external-cavity laser diode devices; however suitable monolithic devices have only achieved linewidths in the range of 1 to 10 MHz. A more complete discussion of the systems requirements and the current state of the art for narrow-linewidth laser diodes is given in the Appendix.

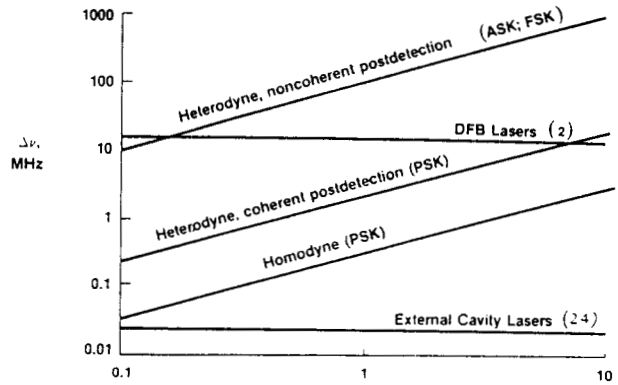

Modulation format	HE/NP ASK, FSK	HE/NP DPSK	HE/CP PSK	Homodyne PSK
R_b = 100 Mb/s	9 MHz	165 kHz	226 kHz	31 kHz
R_b = 1 Gb/s	90 MHz	1.65 MHz	2.26 MHz	310 kHz

1. Laser linewidth requirements for coherent communications systems.[1]

In an analysis of a number of designs, including both distributed feedback (DFB) distributed-Bragg-reflector (DBR) lasers, we have developed a design on an InGaAs multiple-quantum well (MQW) DBR laser with an integrative waveguide and MQW modulator. This design incorporates a number of features at the leading edge of semiconductor laser technology that require development. We, therefore, initiated a development effort using a design that would allow us to develop the technologies necessary for this design, while simultaneously demonstrating device results at various stages of the development program. During the first year, we have developed some of the fabrication techniques required for our integrated device structure. A non-quantum-well structure with separate active and low-loss waveguide layers. Incorporation of these low-loss waveguide layers will be a key element in the design of the structure. We have, based on this effort, now

demonstrated a DBR laser structure that can serve as the building block for our narrow linewidth device.

In addition, we have been developing, in parallel, the MOCVD growth of MQW laser structures in the InGaAsP material system. As a result of this effort, we have demonstrated room-temperature operation of InGaAs/InGaAsP MQW lasers. At this point, we are in a position to incorporate the MQW lasers into the DBR laser structure developed during Phase 1 of this program. The incorporation of the MQW structure into the DBR cavity will also automatically allow for the monolithic integration of modulators.

In this report, we first compare various design approaches, and from this theoretical work, present our design approach. Section III then describes the development work carried out during Phase 1 using developmental structures. In this section, we discuss the fabrication issues to be resolved; the processes developed; the development of the materials growth, including MOCVD-grown MQW lasers; and the initial results obtained from the DBR structures fabricated. Finally, in Section IV, we describe the self-heterodyne spectral linewidth analyzer that was constructed at Sarnoff to support this program and show linewidth measurements made on DFB lasers fabricated at Sarnoff.

Section II

LASER LINEWIDTH AND DESIGN

Two monolithically integrated laser designs were originally considered for the basic narrow-linewidth laser structure. These were a long DFB laser and a DBR laser with an extended intra-cavity, passive waveguide section. Previously, under funding from both NASA and Naval Research Laboratory, Sarnoff had developed single-mode InGaAsP DFB lasers operating at 1.3 μm. These devices consisted of both low-power (5-10 mW) ridge-guide DFB lasers and higher-power (15 mW), buried-ridge structures. Both these structures were fabricated using liquid-phase epitaxy, although they are also compatible with vapor-phase epitaxy and MOCVD. To make an experimental comparison of the DFB and DBR configurations, we had initially hoped to make both types of devices by using our existing DFB technology, while simultaneously developing the technology for the DBR devices. However, for two major reasons, we decided to drop the DFB effort. First, as discussed below, from a technical viewpoint there were several reasons to favor the DBR structure, and second, from a pragmatic viewpoint, such a division of efforts was not consistent with meeting the program goals effectively.

To summarize, the technical basis for favoring the DBR structure was two-fold. First of all, the analysis we did of the linewidth of various cavity designs, which is presented below, indicated clearly that extending the cavity with a long passive section was far superior to using an extended pumped region. As is well known, one fundamental way of narrowing the linewidth is to make a longer cavity. However, if the cavity is extended with a region containing gain, the extended region becomes an additional source of noise, thus mitigating the positive effects of the additional length on the linewidth. An extended *passive* section, which can be incorporated easily into a DBR structure and does not add to the noise, is a better alternative.

In order to compare the narrow linewidth performance of DFB and DBR lasers, we analyzed the linewidth of the corresponding cavity configurations without gratings. In particular, we compared the linewidth and efficiency of simple, long laser cavities, as for a DFB laser, to laser cavities extended by means of an unpumped passive section, as in the case of a DBR laser.

The spectral linewidth of diode lasers that arises from the spontaneous emission noise is given by[2]

$$\Delta\nu = \frac{R(1+\alpha^2)}{4\pi I} \tag{1}$$

where R is the spontaneous emission rate, I is the number of photons in the lasing mode, and α is Henry's linewidth enhancement factor that arises because the change in gain associated with a spontaneous emission event is accompanied by a change in refractive index. Based on Eq. (1), there are two basic means of decreasing the linewidth: (1) modify the cavity to decrease the fraction of spontaneously emitted photons in the mode; and (2) alter the material properties at the lasing wavelength in such a way as to decrease α. We will consider these two issues independently. The device design we have developed is based on an optimization of both.

The basic principle involved in decreasing the linewidth by the design of the cavity is to decrease the spontaneous emission rate into the mode while at the same time increasing the modal intensity. We consider here two alternative cavity configurations. The first is to make a uniform long-cavity Fabry-Perot laser by increasing the length of gain material between the facets. The second approach is to extend the cavity length by incorporation of a passive waveguide section. We call this second approach an extended-passive-cavity laser. In both these approaches, the modal intensity is increased by lengthening the cavity. Specifically, the number of photons in the lasing mode for a constant output power increases linearly with the cavity length. The differences in these two approaches become apparent by considering the spontaneous emission rate.

First consider the uniform Fabry-Perot laser, which is analyzed in reference 2. If the cavity losses are dominated by the end (mirror) losses (i.e., the short cavity regime), then the spontaneous emission rate, which is proportional to the gain per unit length, will decrease as 1/L. However, as the cavity is made longer, the mirror losses become small compared to absorption losses in the cavity, and the gain per unit length, and hence the spontaneous emission rate, becomes independent of L. Combining this with the the dependence of I on L, we see that for short cavity lengths, the linewidth should decrease as $1/L^2$, while for long cavities, it will only fall off as 1/L. Figure 2 shows the calculated linewidth of a 1.3-μm InGaAsP laser operating at an output power of 1 mW as a function of cavity length. For this calculation, $\alpha = 5.5$, the spontaneous emission factor $n_{sp} = 1.7$, the internal cavity loss $\alpha_0 = 30\ cm^{-1}$, and the facet power reflectivities are 80%

and 30%. If we restrict the length of the cavity to about 5 mm from practical materials considerations, the minimum linewidth attainable at 1-mW output power is about 1 MHz.

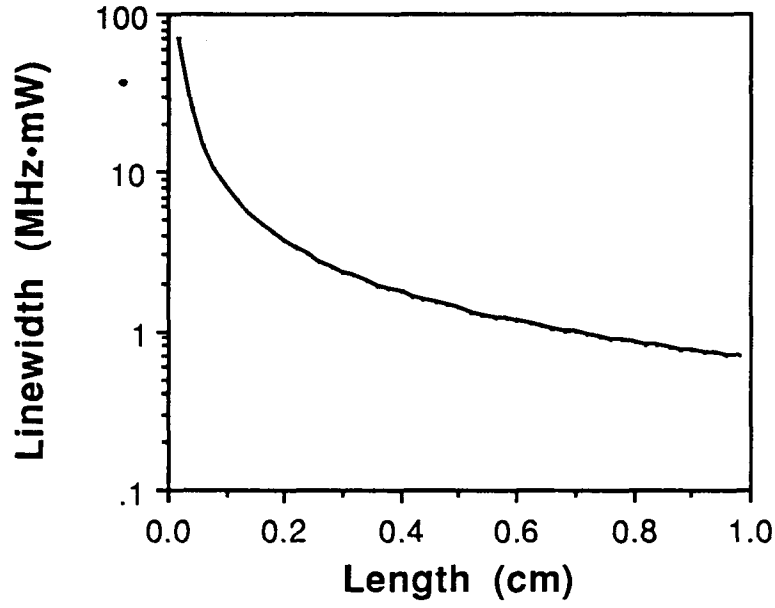

Figure 2. Calculated linewidth of a 1.3-μm Fabry-Perot laser as a function of cavity length.

Based on this linewidth analysis, it should be possible to obtain a 100-kHz linewidth from a 0.5-cm-long uniform Fabry-Perot cavity laser by operating at 10-mW output power. However, by making the device this long, the facet losses become a small fraction of the total cavity loss and, thus, the device becomes extremely inefficient. Figure 3 shows the calculated external efficiency of a uniform-cavity Fabry-Perot laser as a function of length, assuming a 100% internal quantum efficiency and the same parameters as in Fig. 2. The 5% efficiency obtained in an 0.5-cm-long device is too small to obtain 10-mW output power in a single mode. As a result, the minimum linewidth attainable from the device is probably about 1 MHz. Also note that since, for long cavity lengths, both the external efficiency and linewidth-power product are decreasing linearly with increasing length, the minimum linewidth attainable (at the maximum output power) may be independent of length. As a result, little gain in linewidth performance can be expected by increasing the cavity beyond the length for which

the facet losses become small. The minimum linewidth attainable by simply increasing the laser cavity length will therefore be on the order of 1 to 10 MHz.

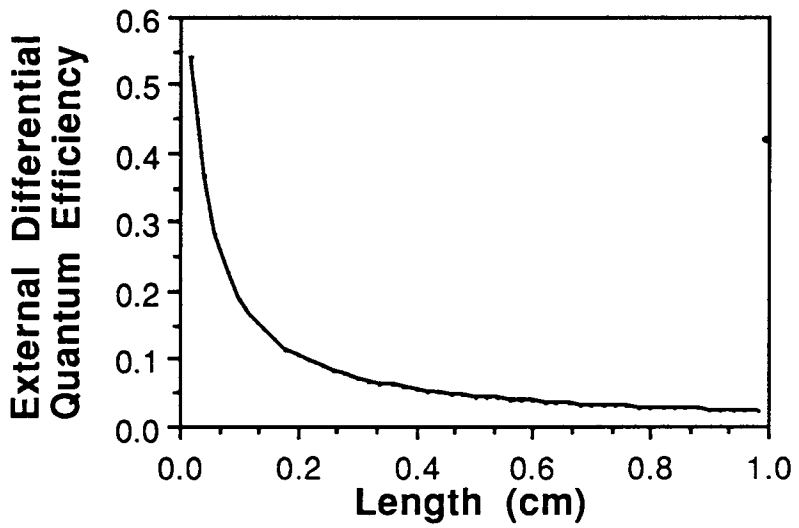

Figure 3. External efficiency of a 1.3-μm InGaAsP Fabry-Perot laser as a function of cavity length.

By using a low-loss passive waveguide instead of a pumped gain section to extend the cavity length, the short-comings of the above approach can be reduced. For a lossless waveguide section of length L_1, the linewidth of the laser decreases as L_1^{-2} for all lengths, and the external efficiency is independent of L_1. It has been shown that the linewidth of an extended-passive-cavity laser with gain and passive region lengths L_0 and L_1, respectively, is reduced by a factor of ξ^2 compared to a uniform cavity of length L_0, where[3]

$$\xi = \frac{L_0/v_{g0}}{L_0/v_{g0} + L_1/v_{g1}} \tag{2}$$

There are two sources of this linewidth reduction. First, the modal intensity in the cavity is increased by the fraction of time the photons spend in the passive section of the cavity; and second, the spontaneous emission rate into the lasing mode is decreased because the density of available modes is increased as ξ^{-1}.

The major issue that must be addressed for a monolithic-extended passive-cavity laser design is the effect of waveguide losses on the linewidth of the device.

We have extended the theory of Henry[3] to include these losses. Figure 4 shows the calculated linewidth of such a laser as a function of passive section length for waveguide power losses (a1 in Figs. 4, 5 and 7) between 0 and 10 cm^{-1}. The gain section length was 300 μm, and all the other parameters were the same as in Fig. 2. For passive section lengths in which the total loss is small compared with the other cavity losses, the linewidth decreases as L^{-2} as expected. As the passive section becomes longer than a few absorption lengths, the required gain, and hence the spontaneous emission rate and the linewidth, increase exponentially with length. At a cavity length of 0.5 cm, a linewidth of about 1 MHz at 1-mW output power can be obtained with waveguide losses of 5 cm^{-1}. This required waveguide loss is well within what can be obtained from high-quality VPE or MOCVD-grown InGaAsP waveguides.

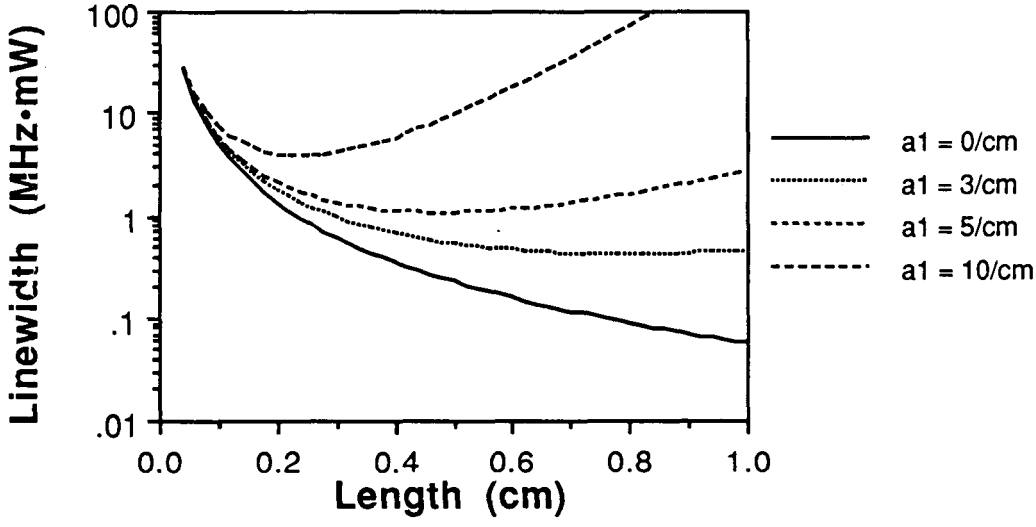

Figure 4. Linewidth of a 1.3-μm InGaAsP extended-passive-cavity laser as a function of the length of the passive section and the waveguide attenuation coefficient a1.

The major advantage of the extended-passive-cavity approach is apparent from looking at the external efficiency, shown in Fig. 5. The efficiency of an 0.5-cm-long device with a 5-cm^{-1} waveguide loss is roughly four times greater than the uniform cavity laser of the same length. This will translate roughly into a four-fold decrease in the minimum linewidth. Linewidths on the order of a few-hundred kHz can therefore be expected from this device.

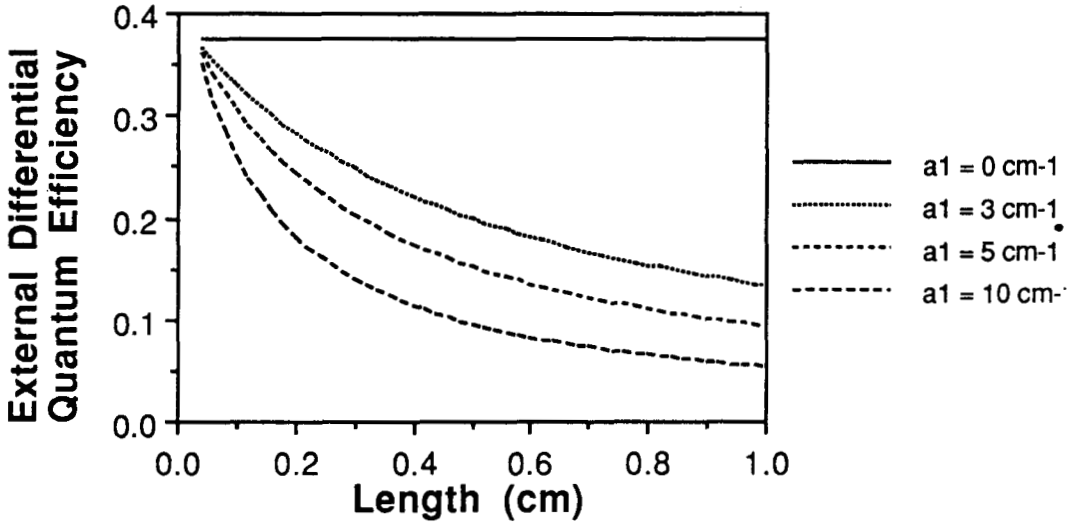

Figure 5. External efficiency of a 1.3-μm InGaAsP extended-passive-cavity laser as a function of the length of the passive section and the waveguide attenuation coefficient a1.

A further reduction in the linewidth of semiconductor lasers can be obtained by reduction of the linewidth enhancement factor, α. Two methods have been demonstrated. The first is to tune the lasing wavelength to the short-wavelength side of the gain peak. Figure 6 indicates the range of values of α that have been obtained in several experiments in which the detuning of lasing wavelength was varied. Reductions in α as large as a factor of 2 have been demonstrated by detuning the lasing wavelength by 15 to 20 nm.[4-7]

A substantial reduction in α has also been reported in both AlGaAs and InGaAsP lasers by using MQW active regions.[8,9,10] For work at 1.3 μm, one group has demonstrated a reduction in α from 5.6 to 3.4 when comparing InGaAsP double-heterostructure and MQW lasers.[8] The effect of this reduction can be calculated easily. Figure 7 shows the calculated linewidth of an extended-passive-cavity InGaAsP MQW laser as a function of cavity length for various waveguide losses, using $\alpha = 3.4$. This analysis indicates that sub-megahertz linewidths are possible at 1-mW output in an 0.5-cm-long device with passive waveguide losses less than about 5 cm^{-1}.

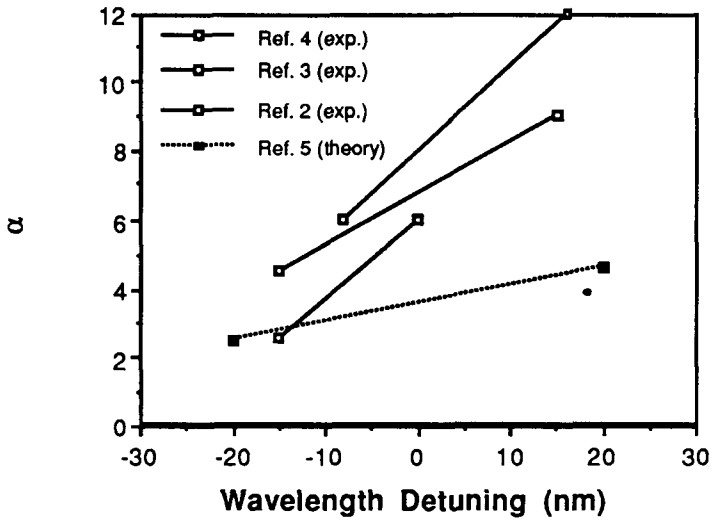

Figure 6. Linewidth enhancement factor in double-heterostructure diode lasers as a function of the laser detuning from the gain peak.

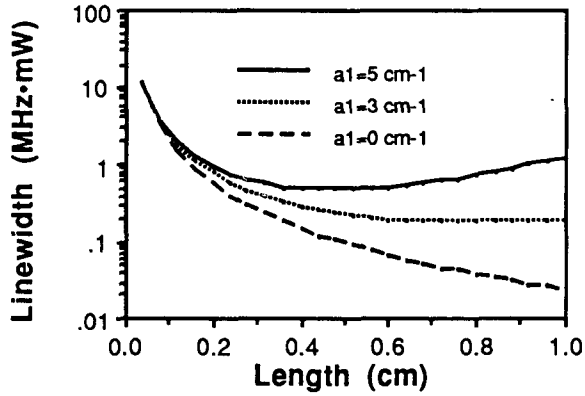

Figure 7. Linewidth of an InGaAsP MQW (α = 3.4) extended-passive-cavity laser as a function of the length of the passive section and the waveguide attenuation coefficient a1.

Based on the above analyses, it is clear that for narrow linewidth applications, an extended-passive-cavity design has a definite advantage over a single, long active gain section. Although this modeling was done only for lasers relying on facet reflection for feedback, the general arguments presented are applicable to DFB and DBR laser design. The design strategy we favor for a monolithic narrow linewidth laser is, therefore, an extended-passive-cavity DBR

laser, as shown schematically in Fig. 8. It consists of a relatively short (200 to 300 μm) MQW gain region coupled to a low-loss passive waveguide 1 to 5 mm in length. DBR is then formed on this passive section to provide frequency selective feedback and to ensure single-mode operation.

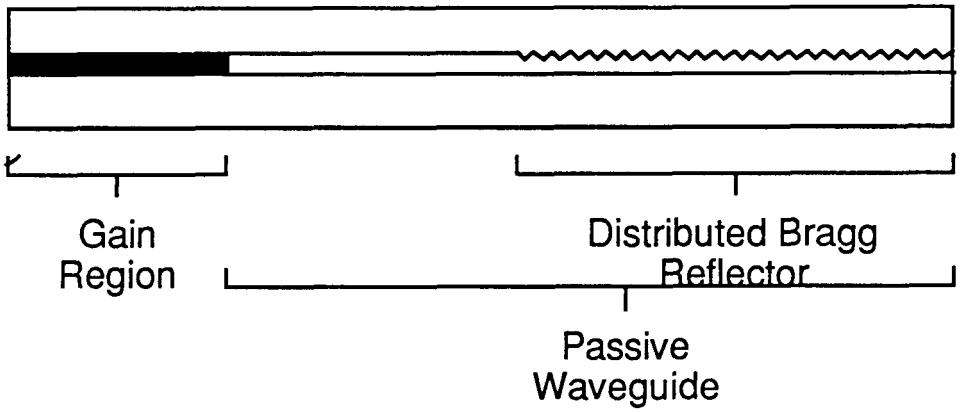

Figure 8. Design concept for a narrow-linewidth, extended-passive-cavity DBR laser.

A second advantage of using a DBR section is that since the Bragg reflector is highly dispersive, it can also help to narrow the linewidth. This additional narrowing occurs because, on one side of the Bragg resonance the variation in gain with oscillating frequency counteracts the effects of the linewidth enhancement factor.[11] With waveguide losses in the passive section < 5 cm^{-1}, linewidths of 100 kHz should be possible with this design.

All of the elements of the monolithic narrow-linewidth laser design shown in Fig. 8 have been demonstrated. This includes InGaAsP and InGaAs MQW lasers, first-order Bragg reflectors at 1.3 and 1.55 μm, and waveguides with loss below 1 cm^{-1}. What has not been demonstrated, however, is the integration of low-loss waveguides with the laser structures. A number of DBR laser structures have been demonstrated, however, no particular effort has been made to reduce the passive region losses below the 10-cm^{-1} level that is typical of the highly doped materials used in laser structures. What is required to realize linewidths of 100kHz from this structure, therefore, is the development of the technology to integrate gain and low-loss waveguide materials without introducing large coupling losses between the different regions.

In addition to the linewidth, the DBR laser design in Fig. 8 has the capability for a wide wavelength tuning range, as would be required in

wavelength division multiplex coherent communications systems. To obtain a wide tuning range without mode hopping, a multiple electrode configuration can be used in the following manner. An electrode on the reflector section controls the feedback wavelength from the Bragg reflector by varying the index of refraction in that region. As the Bragg reflector is tuned, the lasing wavelength changes in such a way that the total round-trip phase delay in the cavity is an integral number of 2π. Since the phase delay due to propagation in the cavity changes with wavelength, the phase change from the reflection must also change to maintain the round-trip oscillation condition. Thus, the lasing wavelength relative to the Bragg condition will, in general, change, and after some tuning range, the laser will jump to a mode closer to the Bragg condition. To eliminate this mode hopping, a second electrode is placed over a passive section of the cavity to maintain a constant propagation phase delay in the cavity as the reflector is tuned. Finally, a third electrode over the gain section is included so that a constant power level can be maintained as the wavelength is tuned. Using such a multiple electrode tuning configuration, continuous tuning over 550 GHz has been reported at 1.5 μm.[12]

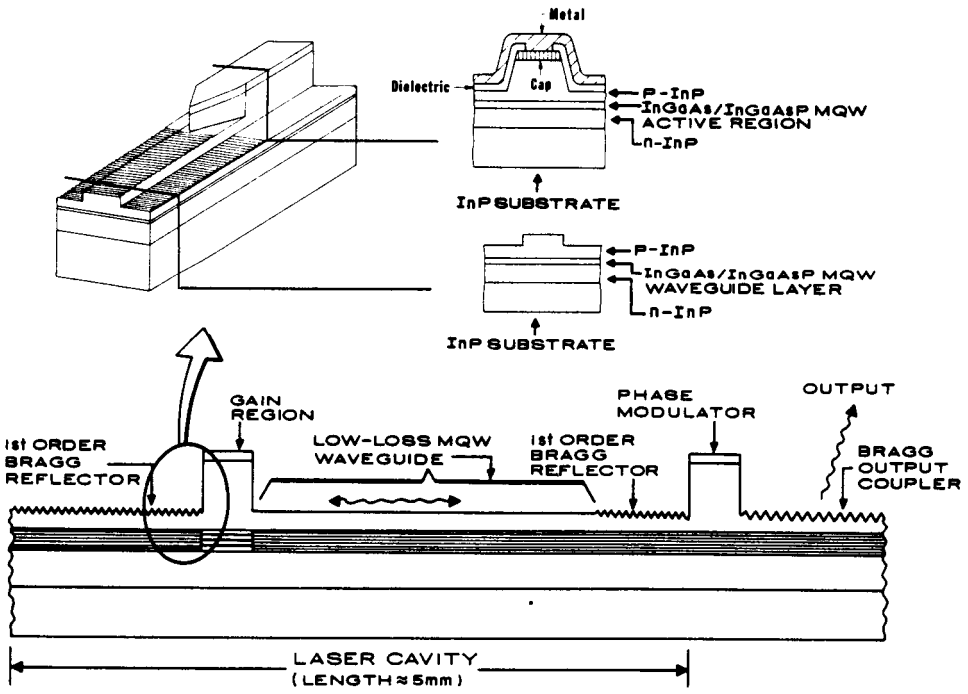

e 9. Monolithic narrow-linewidth InGaAs/InGaAsP/InP MQW laser with phase modulator.

A more detailed schematic drawing of our narrow-linewidth laser design that incorporates a MQW modulator is shown in Fig. 9 and summarized in our design approach. Conceptually, narrow-linewidth operation is obtained by extending the cavity length using a long low-loss waveguide section, which, as shown in the drawing, could be a MQW waveguide structure. In this device, a MQW gain section is used, which results in a reduction in the linewidth enhancement factor and, therefore, a narrowing of the linewidth by a factor of two to four compared to double heterostructure lasers. The feedback for lasing is provided on both ends of the cavity by first-order DBRs. Using grating reflectors eliminates the need for facets, enabling monolithic integration. Furthermore, the grating reflectors can be used in two ways to reduce the linewidth. First, if the grating is tuned to force lasing on the short wavelength side of the gain peak, the linewidth enhancement factor will be reduced. Second, the dispersive nature of the reflection from the grating works to narrow the linewidth in the same way that the material dispersion affects the linewidth enhancement factor. Outside of the cavity, the laser is coupled along a waveguide to an MQW absorption or phase modulator and then to a Bragg output coupler. Using the quantum-confined Stark effect, an efficient modulator can be obtained. By taking the light output through a grating coupler, any feedback into the laser cavity that could upset the narrow linewidth operation under modulation is eliminated. Other methods could also be used for eliminating feedback, such as angled facets.

Two embodiments of this narrow-linewidth laser design that address the problem of integrating InGaAsP material suitable for laser diodes with material suitable for low-loss waveguides are shown in Figs. 10 and 11. The first of these, shown in Fig. 10, is a separate-confinement-heterostructure (SCH) MQW-DBR laser in which the SCH-MQW structure is common to all the sections of the device (gain section, passive waveguides, and modulator). The lateral index guiding can be provided by a ridge waveguide in all sections, as is depicted in Fig. 10.

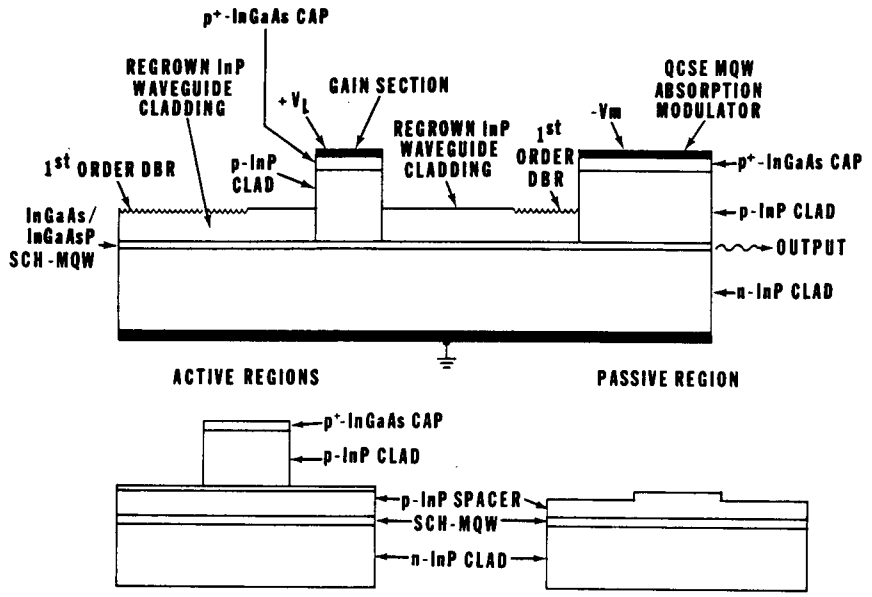

ıre 10. Extended-cavity InGaAs/InGaAsP/InP MQW-SCH DBR laser structure.

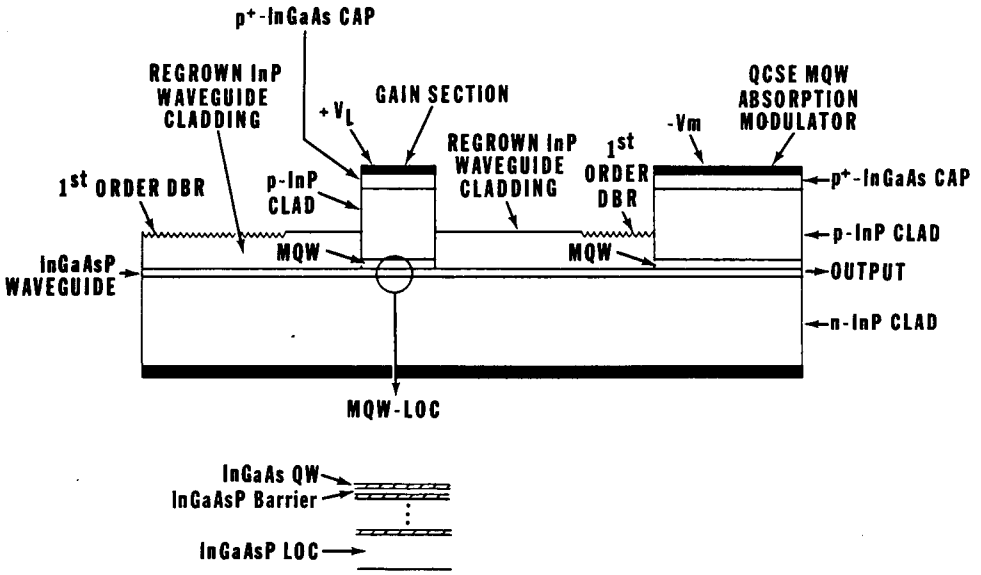

11. Extended-cavity InGaAs/InGaAsP/InP MQW-LOC-DBR laser structure.

SCH-MQW-DBR device has a number of advantages from the of power, efficiency, modulation, and linewidth. First, because the guide structure is common to the entire device, losses at the

transitions between the gain, passive, and modulator sections are virtually eliminated. This will result in lower thresholds, higher output power and, hence, narrower linewidth operation. The common structure is made possible by the fact that in the MQW structure the absorption is small in the unpumped sections. This small absorption arises from three effects: (1) a small confinement factor in the InGaAs wells, (2) saturation of the QW absorption at low intensities, and (3) bandgap shrinkage in the pumped gain region, which shifts the laser emission to longer wavelengths. In the modulator, the QWs allow very efficient, high-speed amplitude modulation through the use of the quantum-confined-Stark effect (QCSE). As a result, the modulator can be relatively short. The speed of modulation is limited only by the junction capacitance, so that bandwidths of several GHz are expected for this ridge-guide device. This QCSE absorption modulator will be suitable for use with an ASK modulation format.

The major risk in this design is that, despite the reasons cited above, the waveguide losses in the MQW passive region may be too high to obtain the linewidth goal of 10 to 100 kHz. Current results in the literature indicate that this loss will be on the order of 10 cm^{-1}. While this is tolerable for many device applications, our modeling indicates that this loss would not allow linewidths much below 1 MHz.

Because the residual losses in the QWs may be unacceptably high, we prefer the design in Fig. 11 in which the MQW active layers in the passive region are removed by etching. The resulting structure, which we call the LOC-MQW-DBR laser, is shown in Fig. 11. In this device, the LOC-MQW structure is first grown everywhere after which the MQW layers are etched away in the passive region, leaving only the transparent LOC layer. InP is then regrown selectively in the passive region to assure a low-loss transition. The same ridge-guide lateral index guiding can be used in this structure, as is shown in Fig. 11. The dimensions for this device are approximately 300 μm for the gain region, 1.5 mm for each of the passive sections, on which 1.0 mm of each has first-order Bragg reflectors, and 1.0 mm for the MQW modulator. The total device length is, therefore, approximately 5 mm.

In conclusion, a design strategy has been developed for monolithically integrated, narrow-linewidth semiconductor lasers. This design consists of a DBR laser in which the cavity has been extended by incorporating a length of passive waveguide. The critical parameter for this device is the loss in the passive waveguide section, since this limits the linewidth that can be obtained. With

waveguide losses below 5 cm^{-1}, linewidths in the range of 100 kHz should be possible from these devices. The realization of this performance level requires lasers and waveguide structures that have already been demonstrated. What needs to be developed is the integration of these devices, which require dissimilar material properties, into a monolithic structure.

Section III

DEVICE DEVELOPMENT

As discussed in Section II, the realization of the narrow-linewidth device approach requires the development of a technology for integrating QW lasers and modulators with low-loss waveguides. In Phase 1 of this program, we have undertaken two major tasks to develop the required technologies. The first of these is to develop the fabrication processes needed for monolithic integration of the DBR structure. As the second major task, we have developed, under internal funding, MOCVD growth of InGaAs QW lasers. Since the MOCVD growth of InGaAsP QW materials is a very new technology, we did not include it in the DBR structure fabricated during the first year. During Phase 1, we therefore used the double-heterostructure LOC DBR (DH-LOC-DBR) laser, instead of the MQW-LOC-DBR, for development of the fabrication. This developmental structure is identical to the MQW-LOC-DBR structure described in Section II except that the MQW active region is replaced by a bulk InGaAsP active region. These structures were grown by hybrid vapor-phase epitaxy, which at the beginning of this program was the most advanced proven growth technology for the required materials. For Phase 2 we planned to combine the fabrication we have developed with a MQW structure to obtain devices with improved linewidth and modulation performance.

DEVICE FABRICATION

The primary issue in the fabrication of a monolithic narrow-linewidth laser the integration of active gain and modulator regions and low-loss waveguides th low-loss transitions between these dissimilar regions. The processes that ıst be developed include the definition of the active and passive regions by hing and also selective regrowth in the low-loss waveguide structures. The hing removes the lossy active region in the passive regions, while the regrowth vides for low-loss transitions, as will be discussed below. These new processes st also be carried out in a manner that is fully compatible with existing ication of the laser structures (a ridge-waveguide laser in this case).

To develop the critical etching procedures, we generated a ridge-guide DBR- laser design, shown in Fig. 12, that requires the same fabrication steps as baseline MQW-DBR structure, but could be fabricated using existing VPE

growth technology, and does not require regrowth. In this way, we have been able to develop a process for etching the passive sections and ridges simultaneously, as required, to demonstrate the integration of gain sections with passive waveguides. With this structure, we were also able to experiment with using a tapered transition region that could obviate the need for the regrowth. For preliminary modulation experiments, an external absorption modulator can be easily integrated in this structure, as shown in Fig. 13. We have used vapor-phase growth (VPE) for this structure because the layer planarity and uniformity, which is critical for these large integrated devices, is substantially better with VPE than with LPE.

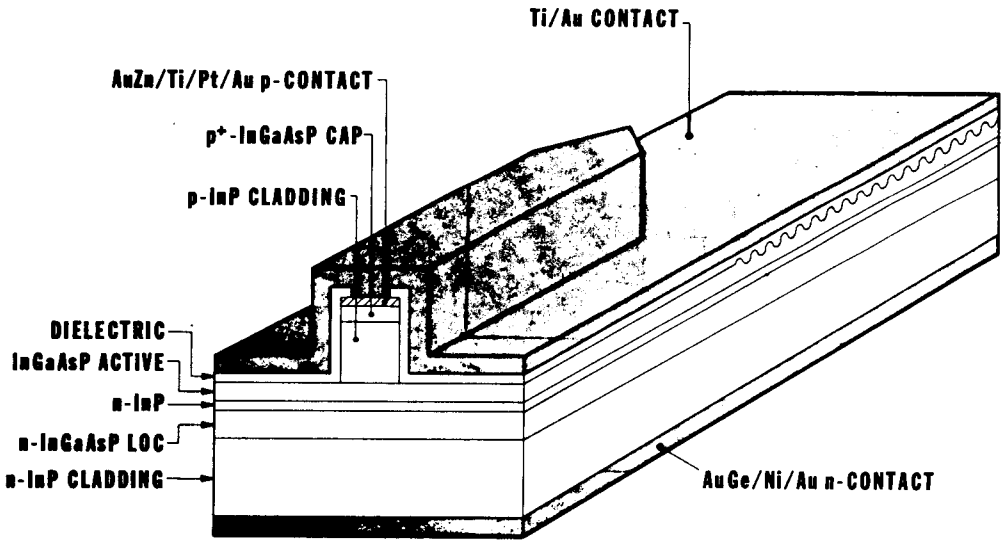

Figure 12. Ridge-guide DH-LOC-DBR laser structure with tapered transition.

The etching of the passive section and the ridge structure required the development of a new hybrid etching technique using dry and wet etching sequentially. Using this combination etching, in which the ridge and passive section are etched together, excellent control was obtained by use of selective chemical etches that stop upon reaching a specific semiconductor layer. The result of etching a ridge using this technique is shown in the 1° angle-lapped cross-section in Fig. 14. First, the ridge is ion-beam etched into the InP cladding layer. Etching of the ridge is then completed using a wet HCl etch that stops at the quaternary layer.

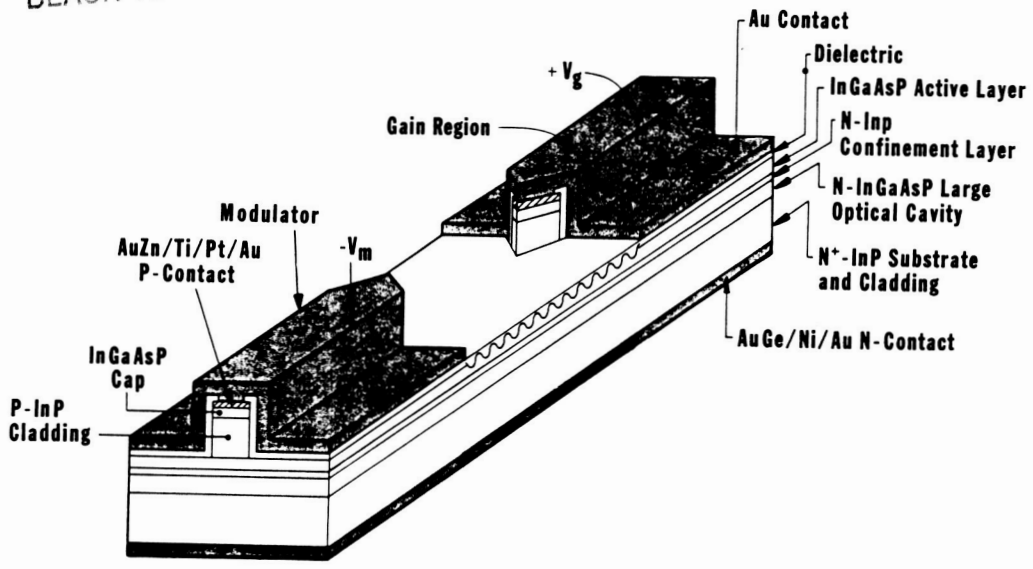

Figure 13. Incorporation of a Franz-Keldysh effect absorption modulator into the DH-LOC-DBR narrow-linewidth structure.

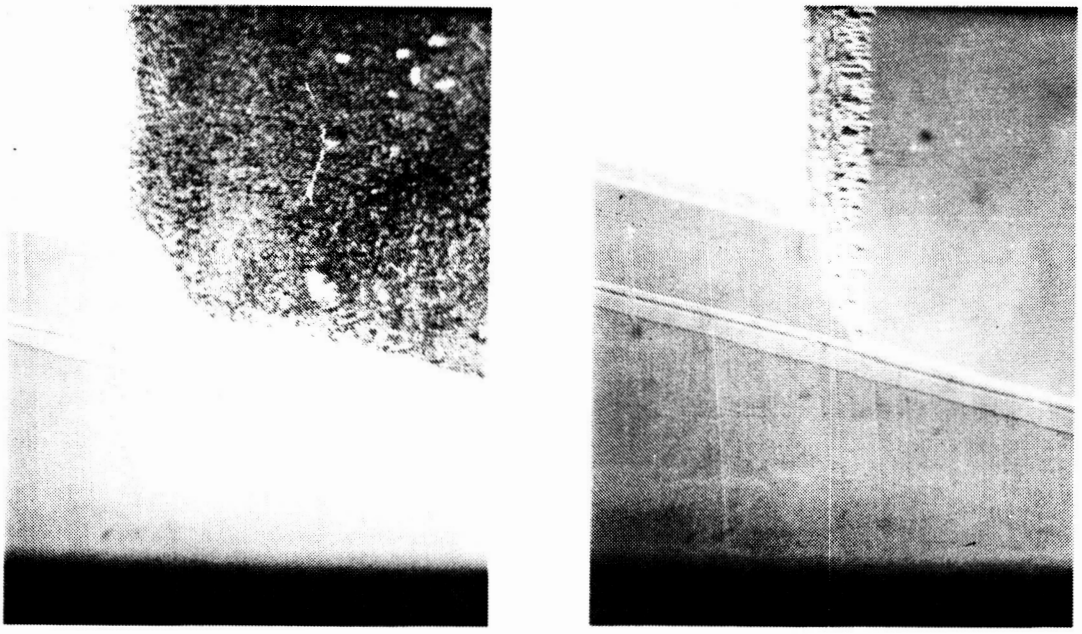

1) After Ion-Beam Etching into InP Cladding

2) After Chemical Etching (Quat. Layer Acts as Etch Stop)

Figure 14. Etching of a ridge-guide InGaAsP laser using ion-beam and selective chemical etching.

For the full DBR structure shown in Fig. 13, the ridge is formed by first ion-beam etching into the InP cladding layer, after which the remainder of the

cladding is removed by etching in HCl. In this structure, the HCl etches only InP and stops at the top of the active layer. The result of using these stop etches is that the etching times are not critical since the grown layers determine the extent of the etching, thus providing excellent control. Alternatively, the gain sections can be protected after ion-beam etching so that only the passive sections are chemically etched. This protection prevents the active layer from being exposed in the gain regions, which could degrade the device performance. Furthermore, leaving some InP cladding in the wings of the ridge provides for improved lateral index guiding. Figure 15 is an SEM of a device completed using this alternative process, showing the ridge and transition region.

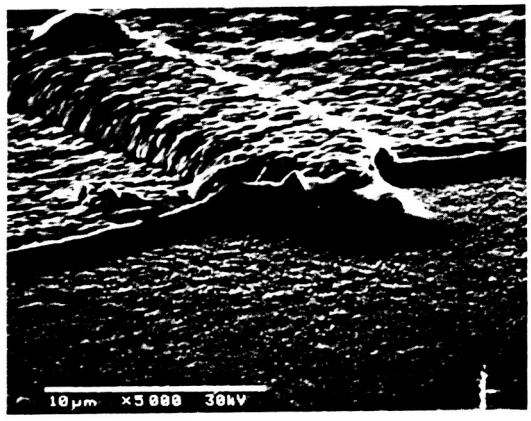

Figure 15. Completed ridge-guide DH-LOC-DBR laser structure in which the gain regions have not been chemically etched.

To develop this etching process we fabricated a number of gain-guided DBR devices, shown in Fig. 16, that did not include a ridge in the gain section. This allowed us to optimize the etching without going through the additional steps necessary to make the ridges. Also, this provided devices on which to test the viability of the tapered transition. Figure 17 shows the P-I curve from one such gain-guided DBR device. The output power is on the order of 5 mW. Figure 18 shows predominantly single-spectral-mode operation of one of these devices, which only occurs in gain-guided devices when the wavelength is locked by the grating feedback. In these first gain-guided DBR-LOC devices, as well as in the first ridge-guide devices, we used a tapered transition to improve the mode matching and coupling efficiency between the active and passive sections. In these devices, however, we typically observed high threshold currents. Further,

as shown in Fig. 19, examination of the near-fields from devices that incorporated second-order gratings, which were fabricated for another program, showed a significant amount of scattered light at the transition. This scattering indicates that the taper was not working as expected, and there was a large discontinuity at the transition.

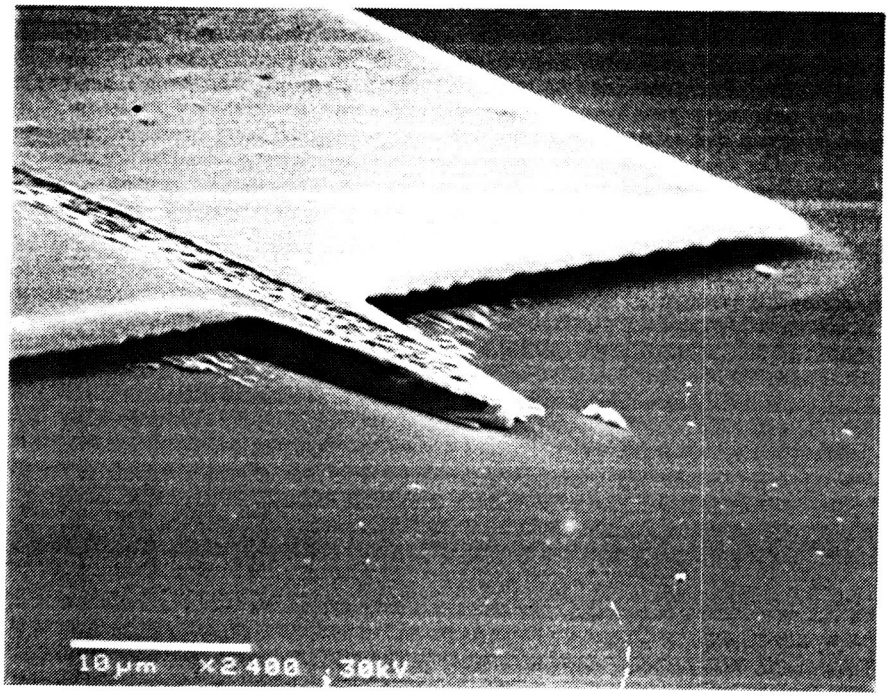

Figure 16. SEM of a gain-guided DBR-LOC laser showing the tapered transition.

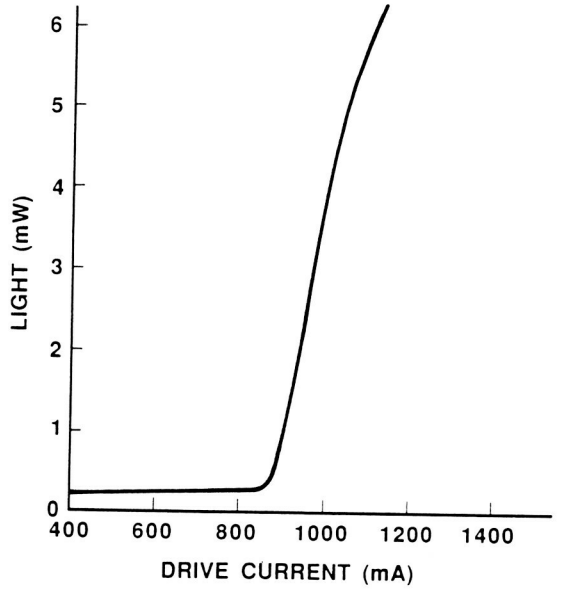

Figure 17. P-I curve from a gain-guide DBR-LOC laser.

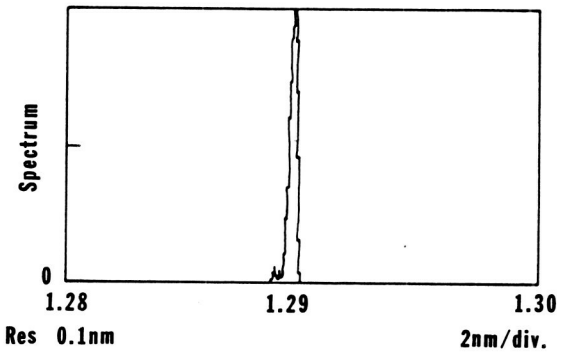

Figure 18. Spectral output from a gain-guided DBR-LOC laser.

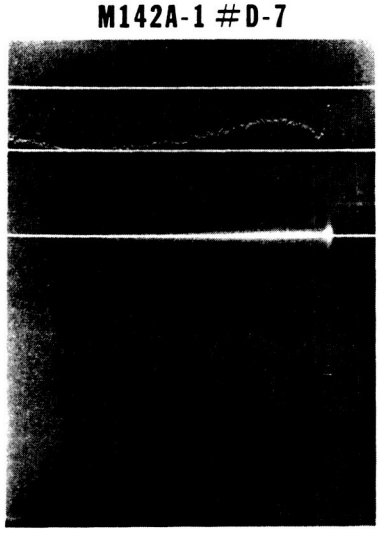

Figure 19. Near-field of a gain-guided DBR-LOC laser with a second-order grating showing scattering at the transition. The top trace is a video slicer output showing the light intensity along the center of the beam.

To reduce the transition losses to an acceptable (and insignificant) level, we determined that a selective regrowth in the passive region after etching is required. This structure, which we call a buried-LOC-DBR is shown in Fig. 20. This structure also includes an additional etch-stop layer above the active layer so that the ridges can be etched using the stop etches we have developed, without exposing the active layer. The significant advantage of the buried-LOC structure is that it is possible to design it with a high transition coupling fraction while still maintaining a large active-layer confinement factor in the gain region. Figure 21 shows the calculated transition coupling fraction and active-layer confinement factor as a function of the LOC (waveguide) thickness for both the LOC (Fig. 12) and buried-LOC (Fig. 20) structures. To obtain a coupling fraction over 70% in the

LOC structure, it is necessary to both leave the active layer in the passive section, and reduce the confinement factor below 20% by increasing the thickness of the waveguide. The result is an increase in both the absorption losses in the passive region and the transition losses. In the buried-LOC structure, the same coupling can be obtained with a confinement factor of 30% and without active-layer losses in the passive region, thus leading to as much as a 50% reduction in threshold gain.

Under a separate program, we have now demonstrated the use of selective regrowth for improving the transitions. As in the DBR-LOC structure, the cap, cladding, and active layers were etched in the passive region using the InP confinement layer as an etch stop. After masking the active region with SiO_2, a 3000-Å InP layer was regrown selectively in the passive region using hybrid vapor-phase epitaxy. A cross-section demonstrating the results of this regrowth is shown in Fig. 22. An especially attractive feature of the process is that the regrowth is tapered (i.e., it is thickest abutting the gain section). With the tapered regrowth, the coupling in the buried-LOC structure will be over 90%.

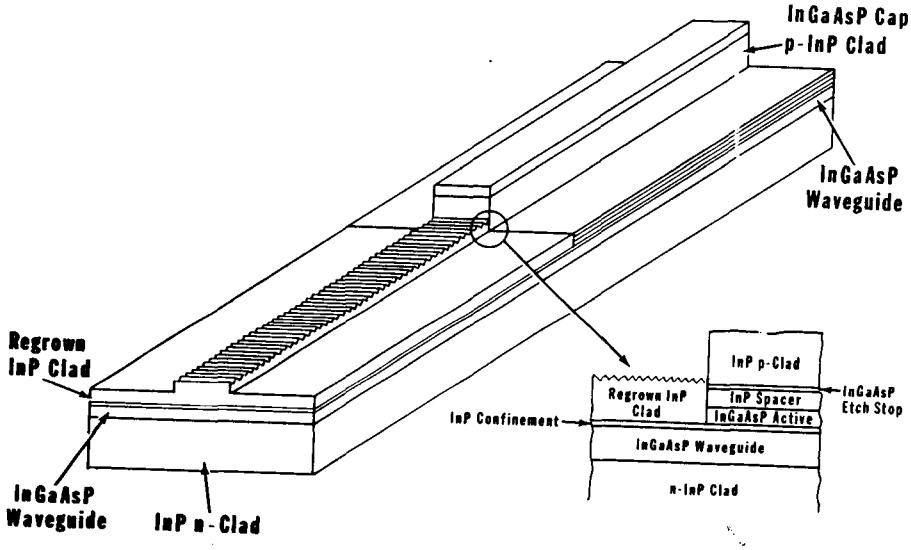

Figure 20. InGaAsP DH buried-LOC-DBR laser structure with additional etch stop layer.

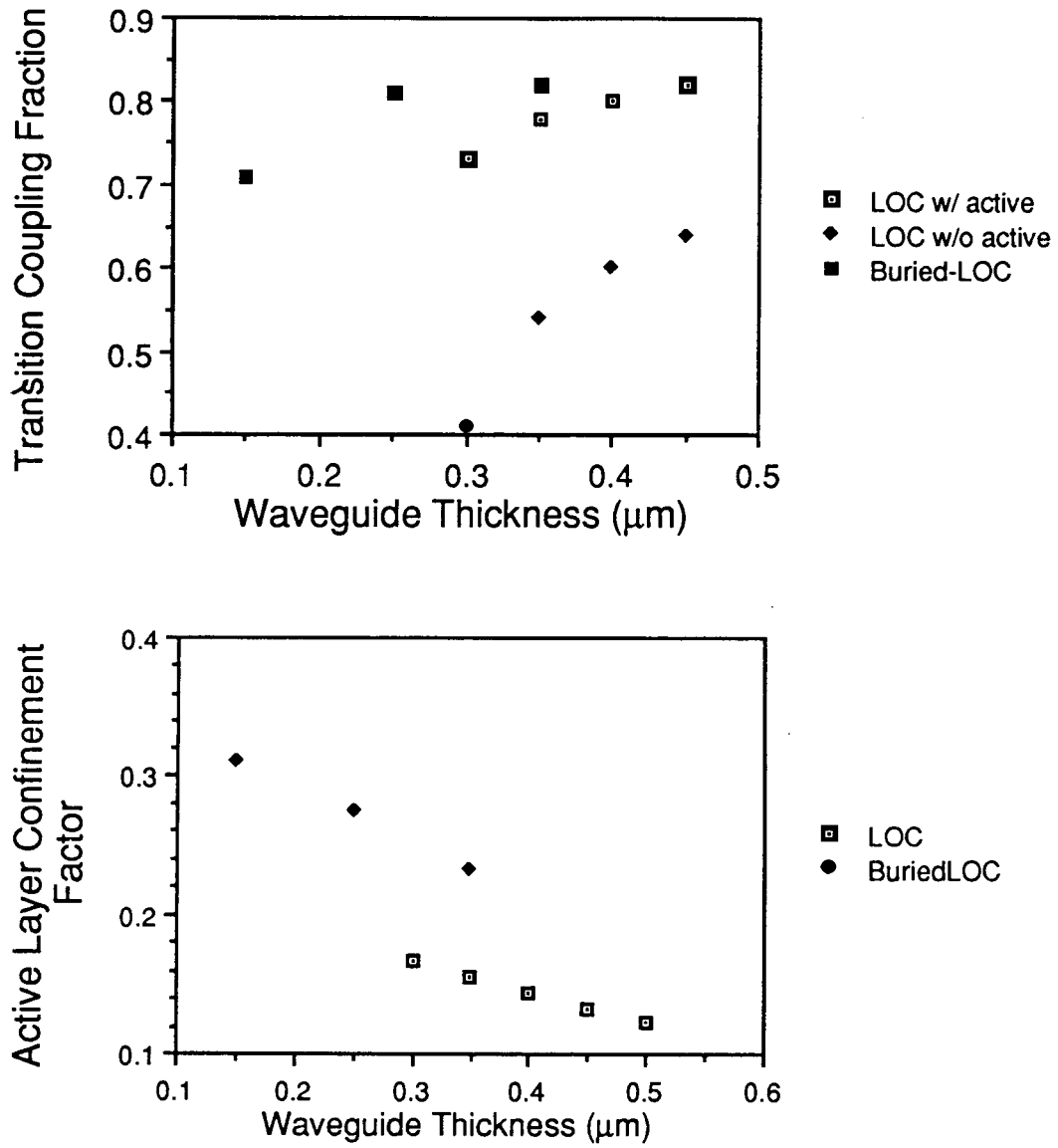

Figure 21. Transition coupling fraction between active and passive sections and active-layer confinement factor for LOC-DBR (with and without active layer remaining in passive section) and buried-LOC structures.

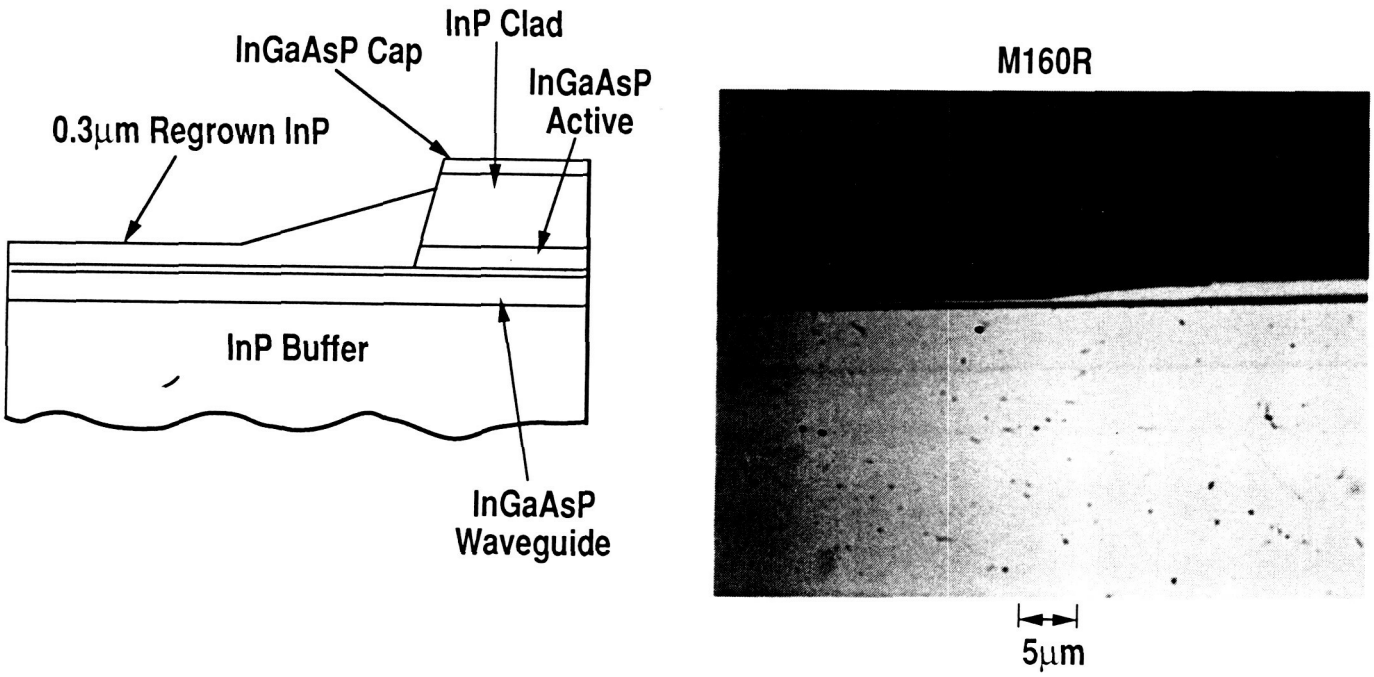

Figure 22. Tapered regrowth of buried-LOC-DBR laser.

Although this buried-LOC structure was not developed until nearly the end of this program, we have now used this structure to make grating-surface-emitting (GSE) DBR lasers using the structure shown in Fig. 23 (using second-order gratings). Using this buried-LOC structure, we have observed linear coherent arrays of GSE lasers of three to nine elements. The characteristics of a gain-guided, buried-LOC surface-emitter arrays are shown in Figs. 24 through 26. The far-field and spectrum indicate single-mode and locked (coherent) operation of this array with greater than 20-dB side-mode suppression. Despite the fact that these gain-guided devices had high losses due to diffraction in the passive sections, the threshold current is about a factor of two lower than similar devices that used only tapered transitions. This regrown structure, which will be directly applicable to the MQW-DBR narrow-linewidth lasers, clearly provides a means for coupling the active and passive sections with very low transition losses.

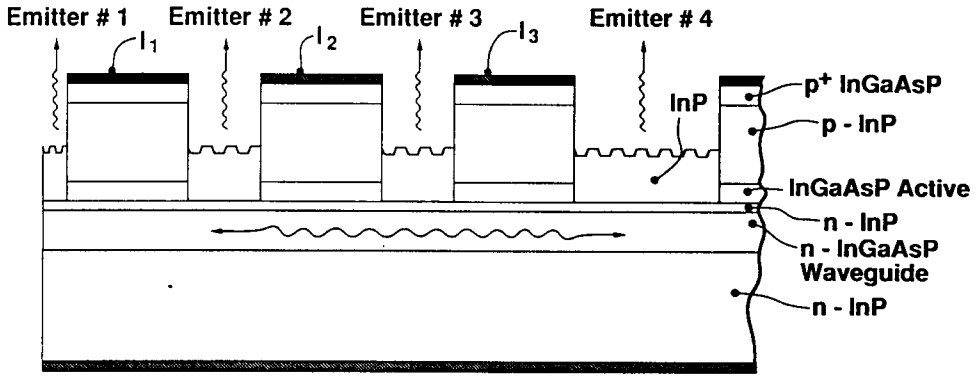

Figure 23. Structure of a three-element, buried-LOC-DBR GSE array.

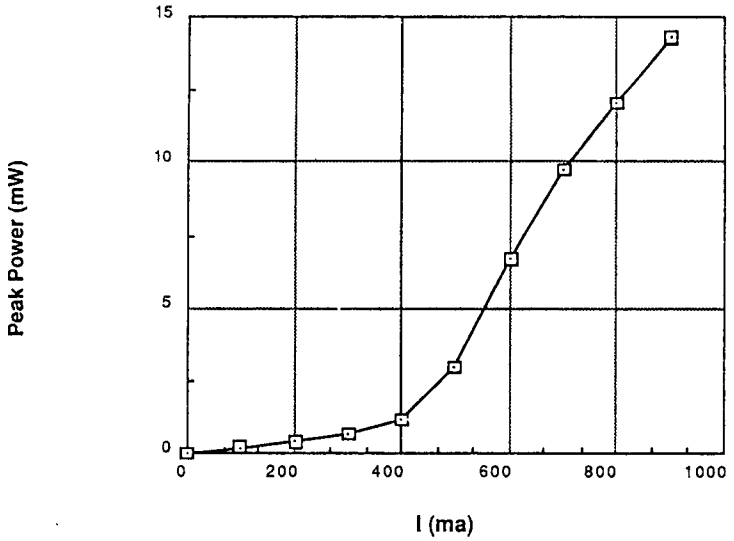

Figure 24. P-I curve from a nine-element, buried-LOC-DBR GSE array.

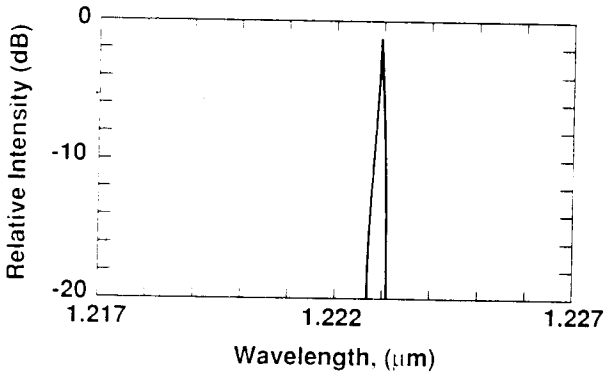

Figure 25. Spectrum of a three-element, buried-LOC-DBR GSE array operating at two times threshold with equal currents to each gain section.

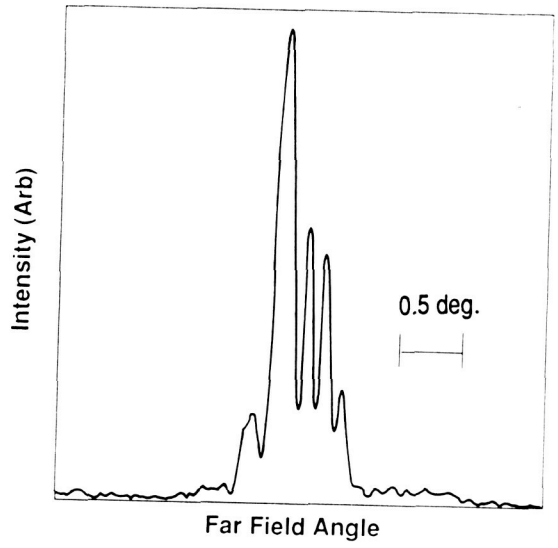

Figure 26. Far-field pattern perpendicular to the grating lines (absolute angle not deteremined precisely) for a three-element, buried-LOC-DBR GSE array under identical operating conditions to Fig. 25.

In addition to the process technology developed to make low-loss transitions in the narrow-linewidth DBR structures, we have also developed the fabrication of the required first-order Bragg reflectors with a 2000-Å period. An SEM micrograph of a 2000-Å period formed on InP is shown in Fig. 27. This grating is fabricated by holographic UV exposure of a photoresist mask followed by ion-beam etching. Controlled etching of the gratings was crucial to device operation because of possible effects on the transitions and low-loss waveguides.

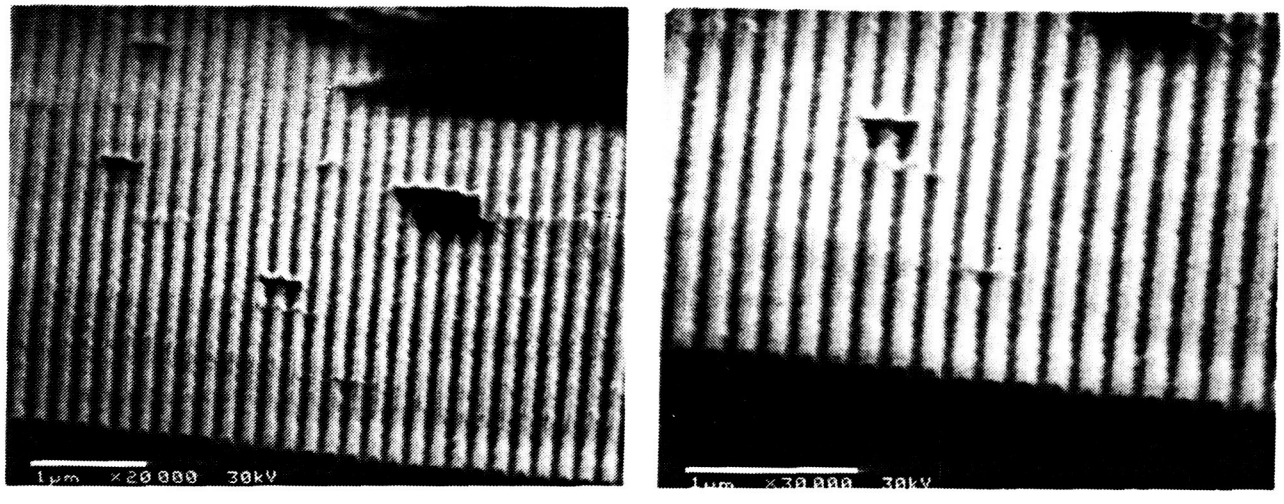

Figure 27. Ion-beam-etched, first-order gratings (period = 2000 Å) fabricated in InP.

B. WAFER GROWTH

The wafer growth carried out during the course of this program consisted of the development of both VPE-growth of the DH-LOC structures and MOCVD growth of InGaAs MQW structures. At the time the program began, VPE was the most advanced proven growth technique available, so it was chosen as the baseline approach for Phase 1, while the development of the MOCVD MQW growth was ongoing concurrently, mostly under internal Sarnoff investment funding. In addition, some additional LPE growth of the DH-LOC structure was done to provide some additional material that could be used in the development of the device processing.

The wafer structure for the InGaAsP DH-LOC that was used both for the simple LOC-DBR and buried-LOC-DBR devices described earlier is shown in Fig. 28. The major issues that had to be resolved in this structure were: (1) the incorporation of more than one type of quaternary layer, (2) the growth of a very thin (> 500 Å) InP etch-stop layer, and (3) obtaining the correct position of the p-n junction.

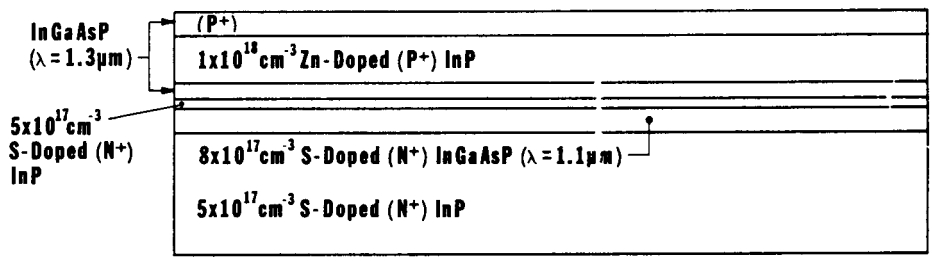

Figure 28. Structure of VPE-grown InGaAsP/InP DH-LOC.

To grow a structure incorporating more than one InGaAsP quaternary composition in a double-barrel VPE reactor requires recalibration of the composition in the InGaAsP barrel during the growth of the wafer (the other barrel is used to grow InP). For this structure, this was accomplished by first growing the InP n-clad, InGaAsP waveguide (LOC) layer (1.1-μm bandgap), and the InP etch-stop layer. At this point, the wafer was withdrawn into the forechamber and the growth conditions in the InGaAsP barrel were modified to grow the 1.3-μm bandgap active layer, and the remainder of the structure was then grown. Once this two-step growth procedure was established, there were no problems with control of the layers or interface quality between the layers. To

verify that this two-step growth was working as desired, and that the thin InP layer was not being etched back, it was necessary to establish a procedure by which the thickness of this layer could be monitored. This was accomplished by developing a staining procedure on angle-lapped cross-sections. An example of this technique on a structure in which the InP etch-stop layer is less than 500-Å thick is shown in Fig. 29. This figure also demonstrates the excellent layer uniformity of thin layers obtained by VPE.. Using this measurement technique, layers < 100-Å thick could be measured optically, which is better than what could be obtained routinely by SEM.

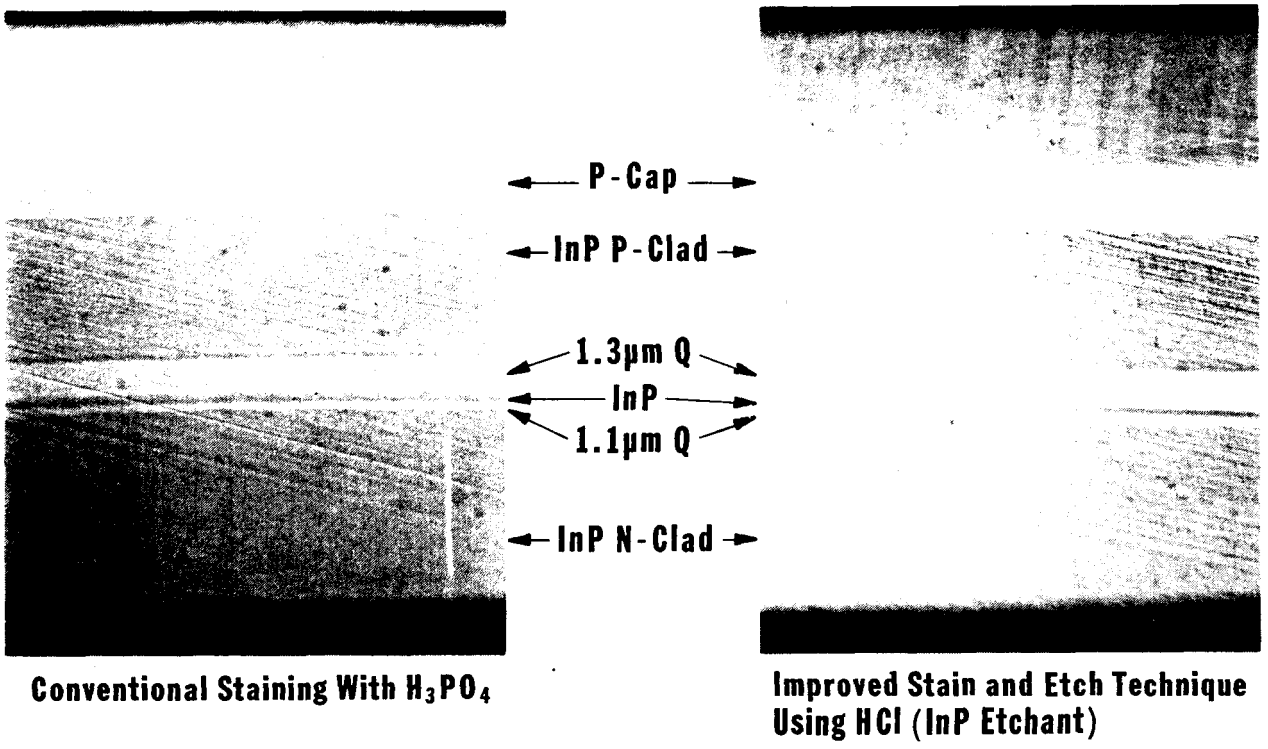

Figure 29. A 1° angle-lapped cross-section of a VPE-grown DH-LOC wafer. The thickness of the InP etch-stop layer is 400 Å.

Perhaps the most difficult parameter to control in both VPE and MOCVD growth of InP-based materials is the position of the p-n junction. This difficulty arises because the Zn p-dopant diffuses during the growth, so that its introduction must be timed so that at the end of the growth it has just diffused down to the active layer. To guide us in the doping for both VPE and MOCVD growth, we have employed a Polaron doping-profile measurement system. An example of a measurement of the doping profile on a DH-LOC structure is shown in Fig. 30.

This figure shows clearly a highly doped cap, a p-InP layer doped at a level of about 1 x 10^{18}, and the n-InP cladding layer doped at a level of about 5 x 10^{17}. Between these two regions is the p-n junction. Furthermore, just to the substrate side of the junction, a region of increased n doping about 0.3-μm wide is visible. This additional peak is due to the InGaAsP waveguide and serves as a marker indicating that the p-n junction is just above the waveguide, i.e., it is in the active layer.

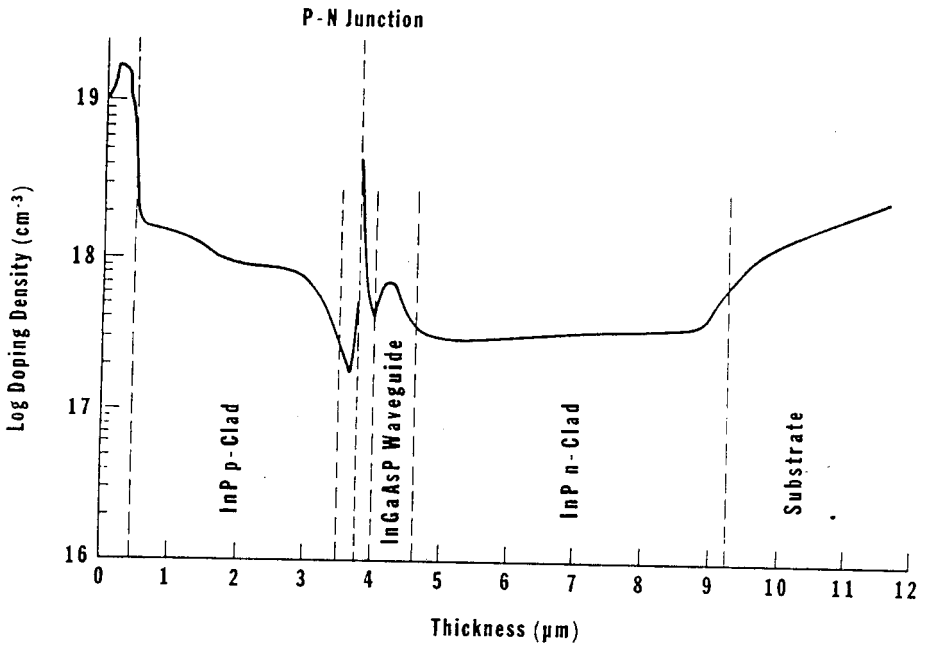

Figure 30. Optimum polaron doping profile from a VPE-grown DH-LOC wafer showing the p-n junction just above the waveguide layer.

Using these techniques to help understand the growth of the DH-LOC structure, we were able to consistently get wafers exhibiting threshold current densities < 3 kA/cm^2, which is excellent for LOC structures with waveguide layers as thick as 0.3 μm. Figure 31 shows P-I curves from a number of broad-area LOC structures taken from one wafer.

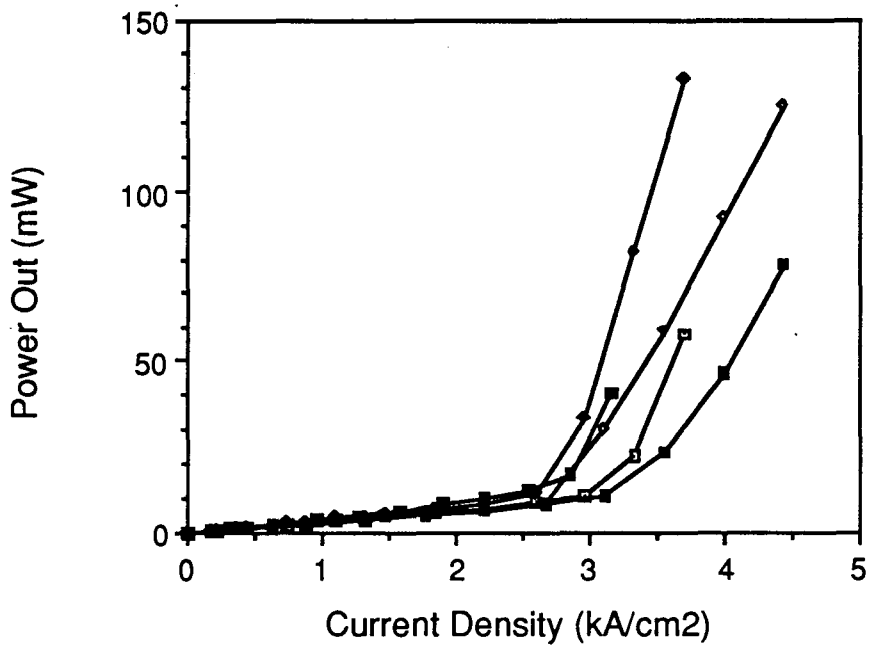

Figure 31. P-I curves for broad-area lasers from a VPE-grown DH-LOC wafer.

To meet the eventual goals of the narrow-linewidth laser design, as well as for other programs, we have been developing MOCVD growth of the InGaAs MQW laser concurrently with the process development for these devices. The eventual design goal is the MQW-LOC-DBR structure in which the InGaAsP active layer used in the DH-LOC-DBR structure is simply replaced by an InGaAs/InGaAsP MQW. All the fabrication that has been developed using the DH-LOC structure will therefore be identical for the MQW structure.

To develop the MOCVD growth techniques of the MQW structures, we have been concentrating on an InGaAsP/InGaAs separate-confinement heterostructure (SCH) MQW in which the SCH structure provides the confinement for the optical field. Using this structure as a benchmark, we have been able to compare our results with what has been grown at other laboratories.

Figure 32 shows a transmission electron micrograph of a InGaAs/InP MQW structure. Excellent layer uniformity and interface quality are evident. A complete SCH-MQW laser structure is shown in Fig. 33, for which the corresponding P-I curve for an 80-μm stripe laser is shown in Fig. 34. The threshold current density for this device was about 1.6 kA/cm^2, which is comparable to the best value of 1.5 kA/cm^2 that has been reported for an InGaAs/InGaAsP SCH-MQW laser.[13] Based on these state-of-the-art results, we

are now ready to begin growth of the MQW-LOC structure for incorporation into the narrow-linewidth DBR device.

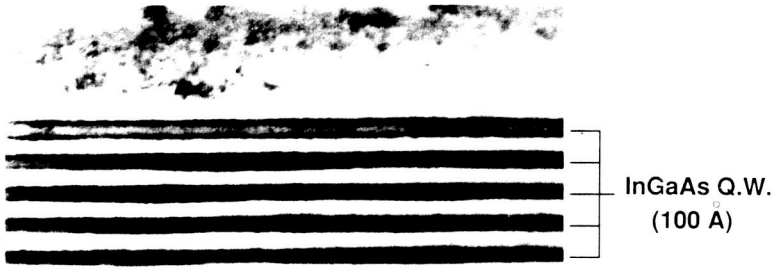

Figure 32. TEM of an InGaAs/InP MQW structure.

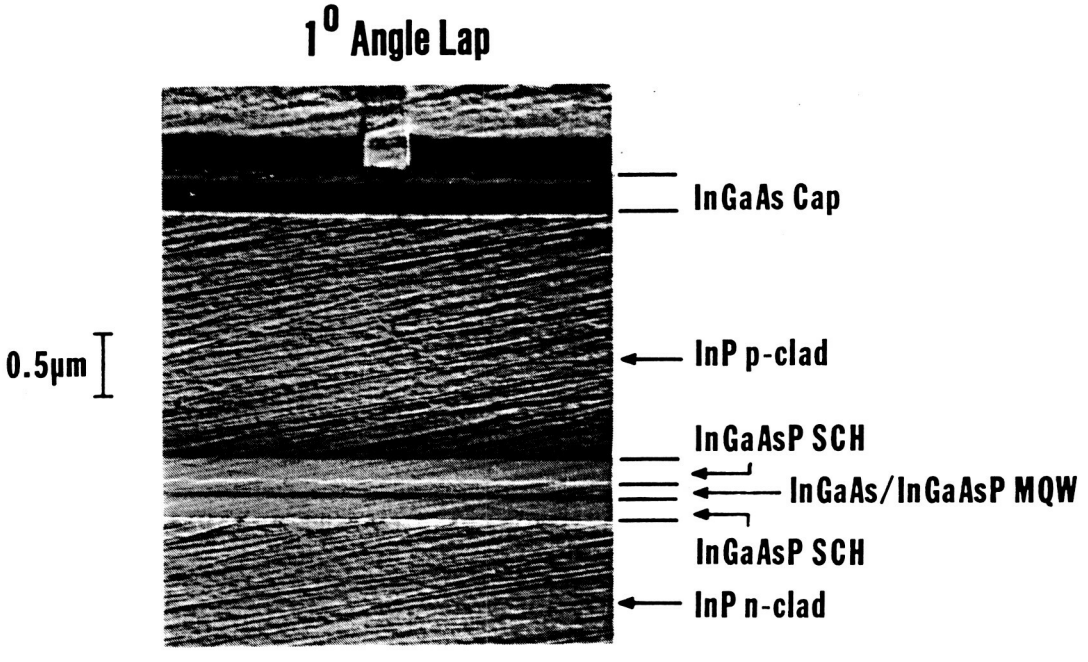

Figure 33. Stained angle-lapped cross-section of an InGaAs/InGaAsP/InP MQW-SCH laser.

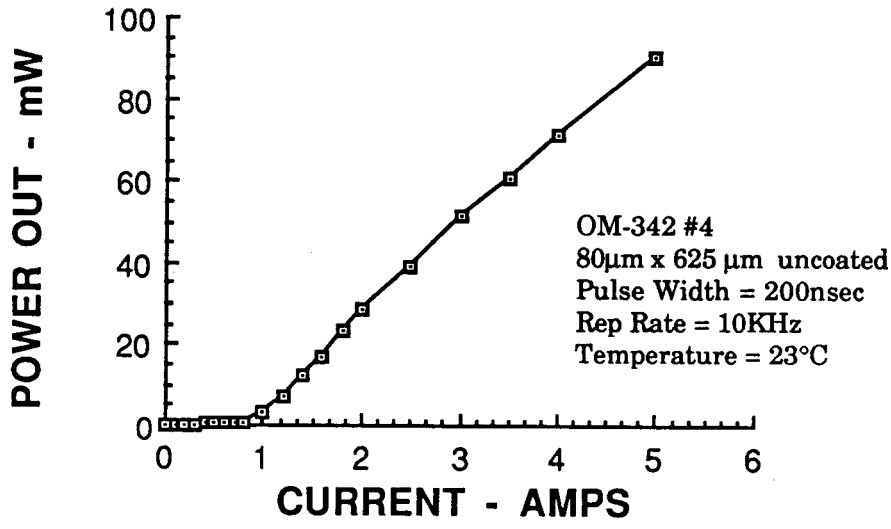

Figure 34. P-I curve for a 625-µm-long, 80-µm stripe InGaAs SCH-MQW laser with a 1.6-kA/cm^2 threshold current density.

Section IV

SPECTRAL LINEWIDTH CHARACTERIZATION

Concurrently with the device development aspects of this program, we have developed the characterization facilities needed for analyzing the spectral properties of narrow-linewidth lasers. Three basic measurement techniques have been developed to characterize spectral linewidth, stability, and noise.

A schematic of the self-heterodyne linewidth analyzer built at Sarnoff is shown in Fig. 35. The linewidth is determined by measuring the linewidth of the beat signal between the laser and a delayed and frequency-shifted version of itself.[14] This system has a resolution of about 10 kHz. The measured linewidth of a buried-ridge DFB laser is shown in Fig. 36. The beat signal is about 30 MHz, indicating a linewidth of about 20 MHz, depending on the exact source of the noise.

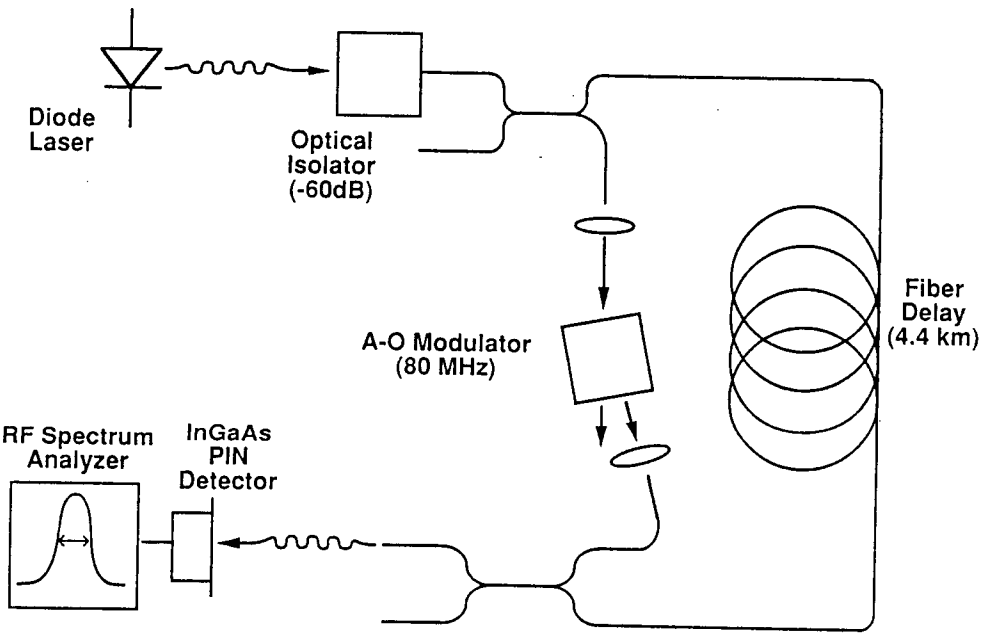

Figure 35. Self-heterodyne linewidth measurement system.

PRECEDING PAGE BLANK NOT FILMED

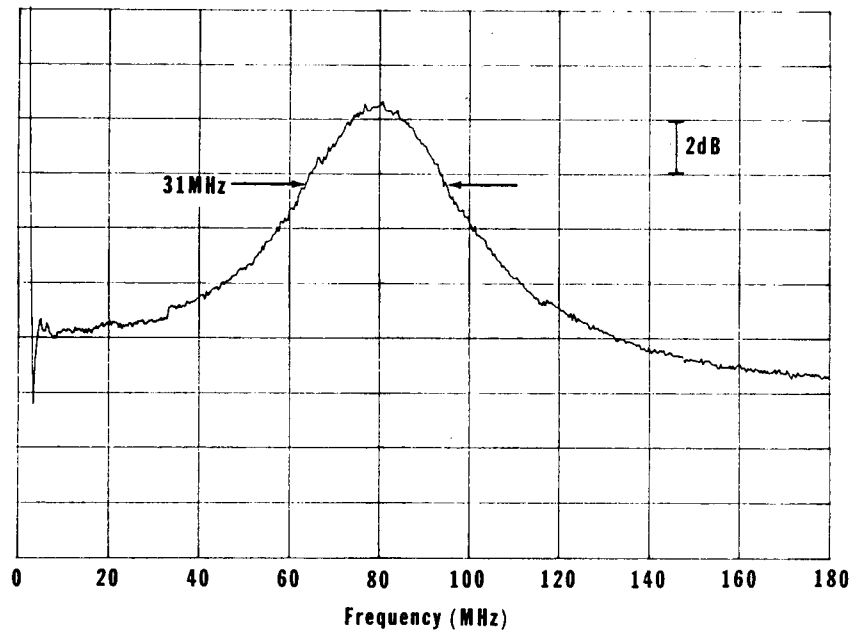

Figure 36. Self-heterodyne measurement of the linewidth of a 1.3-μm buried-ridge DFB laser.

In addition to the linewidth analysis, we have also set up a stabilized high-resolution Fabry-Perot optical spectrum analyzer. This will be used for monitoring the frequency stability of the laser, to the level of about 1 MHz/hour. In addition, this spectrum analyzer can also be used for frequency-noise measurements. The frequency-noise spectrum is required for determining the relative contributions of white and 1/f noise in the linewidth and, hence, determining the noise source in the laser.

Section V

CONCLUSION

In summary, during Phase 1 of this program, we have developed a design for a narrow-linewidth InGaAsP semiconductor laser with an integrated modulator and have developed a number of new fabrication procedures that are required to realize this device. Based on an analysis of a number of designs, including both DFB-DBR lasers, we have determined that a design based on a extended-passive-cavity DBR laser incorporating an InGaAs MQW active region, an integrated low-loss passive waveguide, and an MQW modulator, is the best design for narrow-linewidth operation.

In the Phase 1 of this program, we undertook two major tasks to develop the required technologies for this device. The first of these was to develop the fabrication processes needed for monolithic integration of the DBR structure. As the second major task, we have developed, under internal funding, MOCVD growth of InGaAs quantum well lasers. Since the MOCVD growth of InGaAsP QW materials is a very new technology, we did not include it in the DBR structure fabricated during the first year.

During Phase 1, we therefore used a developmental DH-LOC-DBR laser for development of the fabrication. Based on this structure, we have developed both the etching and regrowth processes required for monolithic integration of active (gain and modulator) sections with low-loss passive waveguides, as well as the fabrication of gratings on InP with periods less than 2000 Å. As a result of this effort, we demonstrated, under a separate program, linear arrays of grating-surface-emitting DBR lasers using our basic narrow-linewidth laser design. Concurrently with this work, we have also demonstrated state-of-the-art InGaAs MQW lasers.

We are now in a position to incorporate the MQW laser structures into the DBR laser structure developed during Phase 1. The incorporation of the MQW structure into the DBR cavity will also automatically allow for the monolithic integration of modulators. Therefore, all the elements required for the proposed narrow-linewidth laser structure are in place.

Section VI

REFERENCES

1. L.G. Kasovsky, "Coherent Optical Receivers: Performance Analysis and Laser Linewidth Requirements," Opt. Eng. 25, 575 (1986)

2. C. H. Henry, "Theory of the Linewidth of Semiconductor Lasers," IEEE J. Quantum Electron. **QE-18**, 259 (1982).

3. C. H. Henry, "Theory of Spontaneous Emission Noise in Open Resonators and Its Application to Lasers and Optical Amplifiers," J. Lightwave Technol. **LT-4**, 288 (1986).

4. K. Kikuchi and H. Iwasawa, "Measurement of Linewidth Enhancement Factor of Semiconductor Lasers by Modified Direct Frequency-Modulation Method," Electron. Lett. **24**, 821 (1988).

5. K. Kikuchi, "Precise Estimation of Linewidth Reduction in Wavelength-Detuned DFB Semiconductor Lasers," Electron. Lett. **24**, 80 (1988).

6. K. Y. Liou, N. K. Dutta, and C. A. Burrus, "Linewidth-Narrowed Distributed Feedback Injection Lasers with Long Cavity Length and Detuned Bragg Wavelength," Appl. Phys. Lett. **50**, 489 (1987).

7. S. Ogita, M. Yano, H. Ishikawa, and H. Imai, "Linewidth Reduction in DFB Laser by Detuning Effect," Electron. Lett. **23**, 393 (1987).

8. Y. Arakawa and A. Yariv, "Quantum-Well Lasers – Gain, Spectra, Dynamics," IEEE J. Quantum Electron. **QE-22**, 1887 (1986).

9. S. Noda, K. Kojima, K. Kyuma, K. Hamanaka, and T. Nakayama, "Reduction of Spectral Linewidth in AlGaAs/GaAs Distributed Feedback Lasers by a Multiple Quantum Well Structure," Appl. Phys. Lett. **50**, 863 (1987).

10. C. A. Green, N. K. Dutta, and W. Watson, "Linewidth Enhancement Factor in InGaAsP/InP Multiple Quantum Well-Lasers," Appl. Phys. Lett. **50**, 1409 (1987).

11. R. F. Kazarinov and C. H. Henry, "The Relation of Line Narrowing and Chirp Reduction Resulting from the Coupling of a Semiconductor Laser to a Passive Resonator," IEEE J. Quantum Electron. **QE-23**, 1401 (1987).

12. S. Murata, I. Mito, and K. Kobayashi, "Tuning Ranges for 1.5-μm Wavelength Tunable DBR Lasers," Electron. Lett. **24**, 577 (1988).

13. A. Kasukawa, I. J. Murgatroyd, Y. Imajo, T. Namegaya, H. Odamoto, and S. Kashiwa, "1.5-μm GaInAs/GaInAsP Graded-Index Separate-Confinement-Heterostructure Multiple-Quantum-Well (GRIN-SCH-MQW) Laser Diodes Grown by Metalorganic Chemical Vapor Deposition (MOCVD)," Electron. Lett. **25**, 659 (1989).

14. T. Okoshi, K. Kikuchi and A. Nakayama, "Novel Method for High Resolution Measurement of Laser Output Spectrum," Electron. Lett. **16**, 630 (1980).

Appendix

Laser Diode Technology for Coherent Communications

D. J. Channin, S. L. Palfrey and M. Toda

David Sarnoff Research Center
Subsidiary of SRI International
Princeton, New Jersey

Introduction

This paper discusses the impact of state-of-the-art diode laser optical characteristics on the overall performance capabilities of coherent communication systems. In it we explore what the present laboratory device performance represents in terms of system capabilities and what issues remain to be resolved in order to achieve certain goals. The paper deals with the following subjects:

- Optical performance issues for diode lasers in coherent systems.
- Reported measurements of key performance parameters.
- Optical requirements for coherent single channel and (especially) multichannel communications systems.
- Limitations imposed by diode laser optical performance on multichannel system capabilities.
- Implications for future developments.

A major interest in coherent systems stems from their long term potential for economically providing massive amounts of bandwidth to end users. Broadband subscriber services, both digital and analog, would be the most important commercial users of such a potential. Tunable multichannel systems based on operational principles similar to radio techniques are an alternative to digital multiplexing and switching approaches, which are now also being considered for such networks. Looking broadly at the technical issues, we ask what such systems would be capable of if current and anticipated laboratory performance were available economically from mature manufacturing technologies.

Optical Performance Issues

Diode lasers are used in optical communications as signal sources and as local oscillators in receivers. As such, the three main optical performance issues are phase noise linewidth, wavelength tuning range, and wavelength stability. Other issues, such as optical power output and modulation frequency capability, while critical for design of specific systems, do not have the general relevance to overall system capability that the first three have. We therefore limit our discussion to these three main performance issues. Also, in focusing on subscriber loop services rather that long distance transmission, we do not include

characteristics of the optical fiber transmission itself that would not be apparent over short links.

Figure 1 shows the results of approximately fifty separate published measurements of semiconductor laser diode linewidth in work directed toward achieving narrow linewidth through various techniques. The data points are grouped by device type: 1. distributed feedback (DFB) lasers, 2. hybrid devices combining DFB lasers and external cavities, 3. monolithic combinations of external cavities and DFB lasers, 4. hybrid devices combining Fabry-Perot (FP) lasers with external cavities, and 5. monolithic devices combining external cavities with FP or distributed Bragg reflector (DBR) lasers. The measured linewidth is plotted against cavity length.

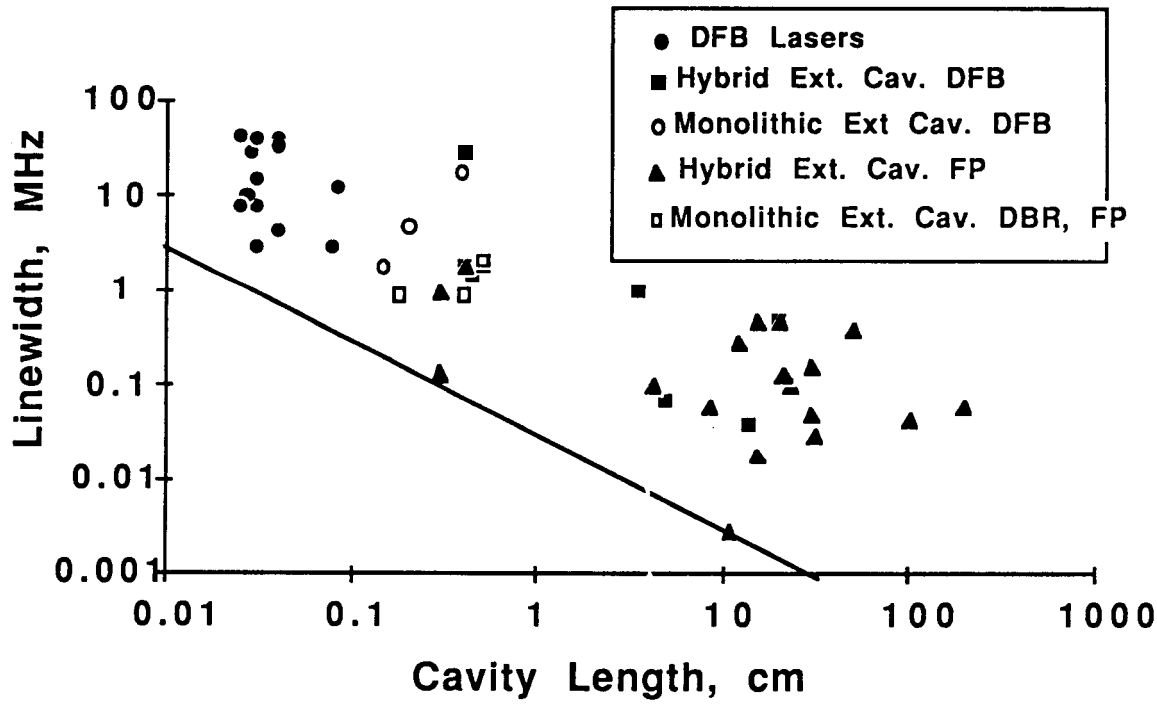

Figure 1. Diode laser linewidth measurements.

The measurement results exhibit a range of four orders of magnitude in observed linewidth. As expected from the theory of laser phase noise induced by optical spontaneous emission, there is a general trend to narrower linewidths with increasing cavity length.[1] Overall, the linewidth appears to be inversely proportional to cavity length, although there is at least an order of magnitude spread in the observed linewidths at any given cavity length. The solid line represents what is apparently the state of the art. Only two points define this limit; most of the reported values are significantly in excess of this line over the entire range of cavity lengths.

We believe that the hopes for economical coherent systems for large-scale use by subscribers will depend on the use of monolithic fabrication approaches. Materials considerations would probably limit cavity lengths in such devices to

less than one centimeter. From Figure 1, this would imply linewidths of about 0.1 MHz at the state of the art, a value that has not yet been approached experimentally in monolithic devices.

A histogram of reported measurements of wavelength tuning range in diode lasers is shown in Figure 2. The upper limit on tuning range is set by the gain-bandwidth product in InGaAsP materials to about 5000 GHz. Useful electronic tuning is limited to 1000 GHz or less by the need to avoid wavelength jumps and maintain constant output power and modulation conditions. Practical tuning in economical systems may be considerably less than the maximum possible in order to simplify the controlling system and to achieve reproducible operation. This is because tuning diode lasers requires simultaneous control of as many as three parameters [2,3]: 1. the optical phase in the laser cavity, 2. the wavelength of the dispersive feedback element, and 3. the pumping level for the gain region.

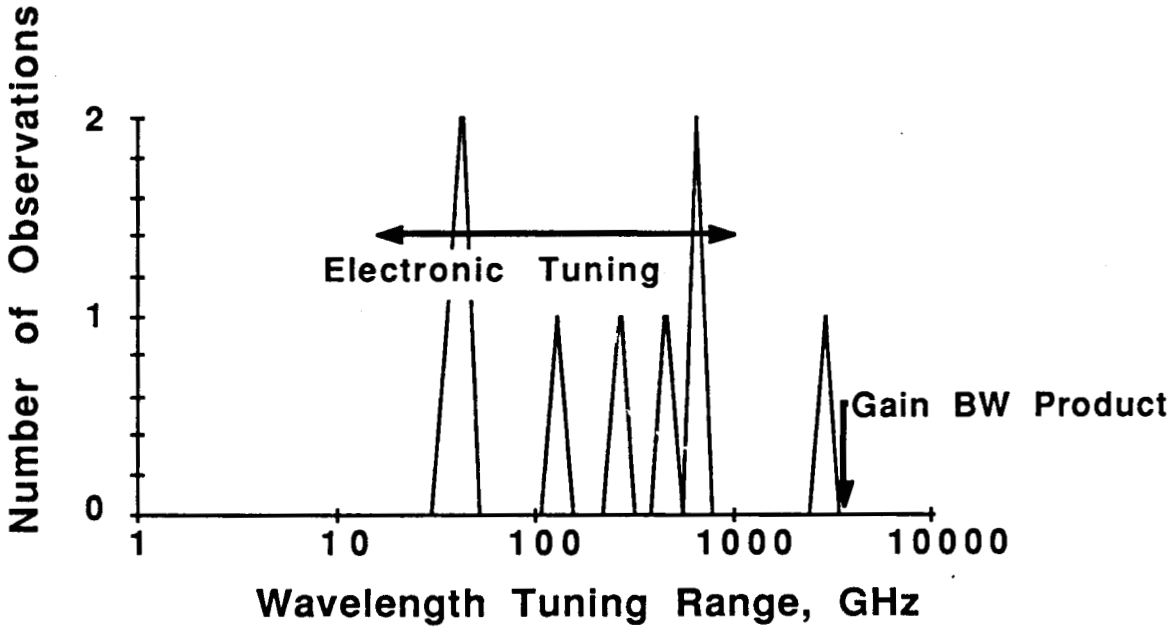

Figure 2. Diode laser tuning range.

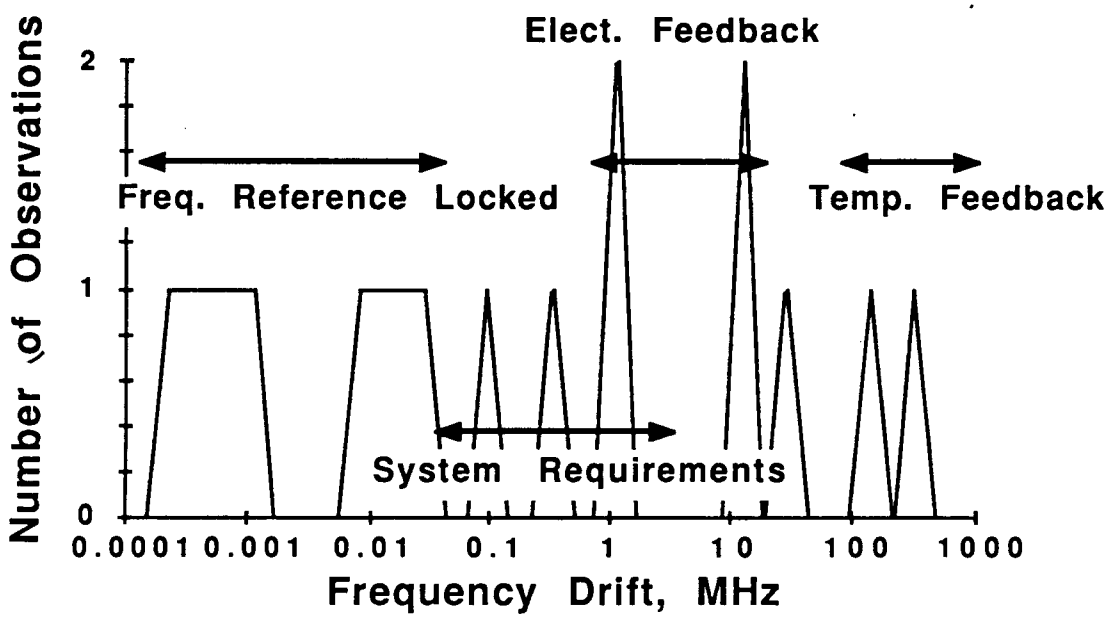

Figure 3. Diode Laser Stabilization Performance.

Figure 3 shows reported performance in stabilizing the wavelength of diode laser operation. This is especially important for multichannel systems, which will require that optical transmission be kept within specified channel bands. The methods for laser stabilization range from temperature control and feedback (the most coarse), electrical feedback (finer), to frequency locking to atomic-level references (the most accurate). Frequency locking may be practical at central office system levels, but is probably uneconomical at subscriber premises or in field operations.

Optical Requirements for Coherent Systems

Single channel coherent systems require specific relationships between laser linewidth and signal bandwidth that depend on the type of modulation. These different signal modulation techniques result in different sensitivity limits [4-6]. Figure 4 shows the required linewidth to signal bandwidth ratio, plotted against the relative sensitivity that could be achieved with various modulation schemes. The modulation approaches shown are homodyne phase shift keying (PSK-HO), heterodyne phase shift keying (PSK-HT), differential phase shift keying (DPSK), frequency shift keying (FSK) and amplitude shift keying (ASK). Generally, the improvement in sensitivity by adoption of the various types of phase shift keying requires a correspondingly narrower laser linewidth. Direct detection sensitivity limits are shown for comparison.

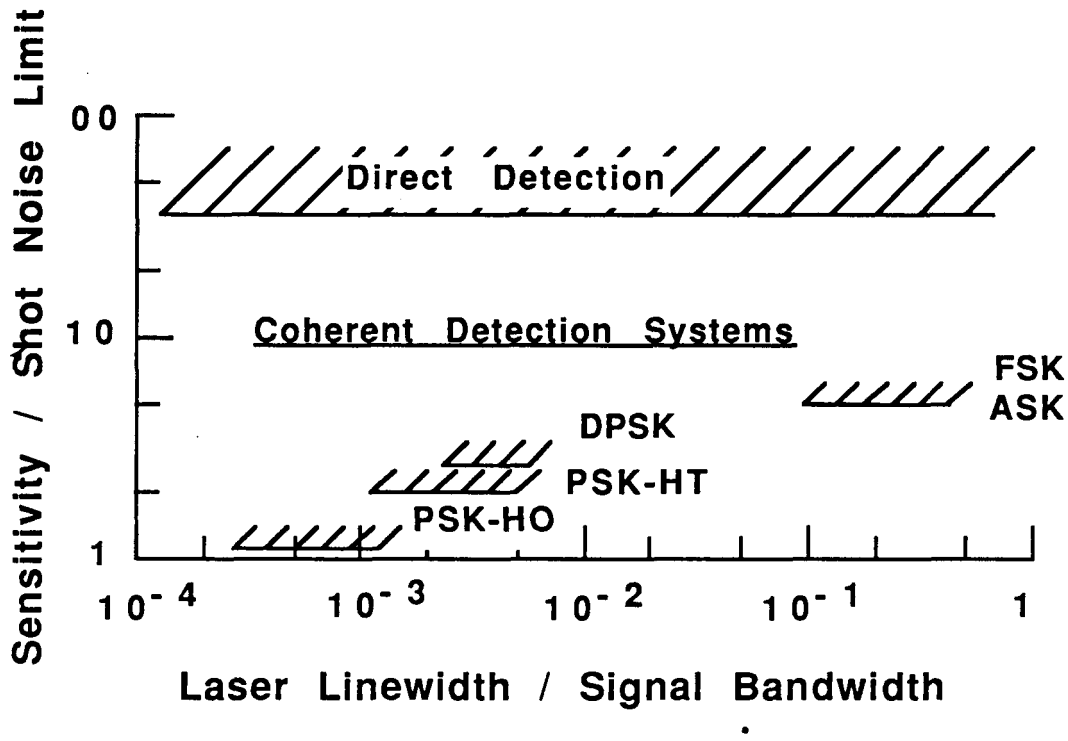

Figure 4. Linewidth requirements for single channel communication systems.

Multichannel transmission capacity is limited by interchannel interference and the tuning range of the laser used for the transmitter and the receiver local oscillator. The number of channels is simply the laser tuning range divided by the full frequency range required per channel to avoid interchannel interference. Such interference can have at least two sources: the information modulated onto the optical carriers and the phase noise introduced by the source laser. In equation form,

$$N_{channel} = \frac{\Delta f_{tuning}}{\Delta f_{mod} + \Delta f_{noise}}$$

For equally spaced channels, the interchannel noise crosstalk depends on the required carrier-to-noise ratio (CNR), the signal bandwidth (B), and the laser linewidth (Δf_{laser}) according to the following expression [7]:

$$\Delta f_{noise} = [\pi \cdot B \cdot CNR \cdot \Delta f_{laser} / 12]^{1/2}$$

The required Δf_{mod} is taken to be five times the channel bandwidth, a relationship representative of the results of various studies [8,9].

Combining these relationships, we have calculated the maximum system channel capacity for various applications. Figures 5 and 6 show the number of

tuned channels for digital and analog video, respectively. These differ in the required carrier-to-noise ratios, taken to be 25 dB for digital and 60 dB for (AM) analog video. These calculations do not take into account the direct (single channel) dependence of CNR on laser linewidth, which may impose additional requirements on laser linewidth, especially in narrowband analog systems.

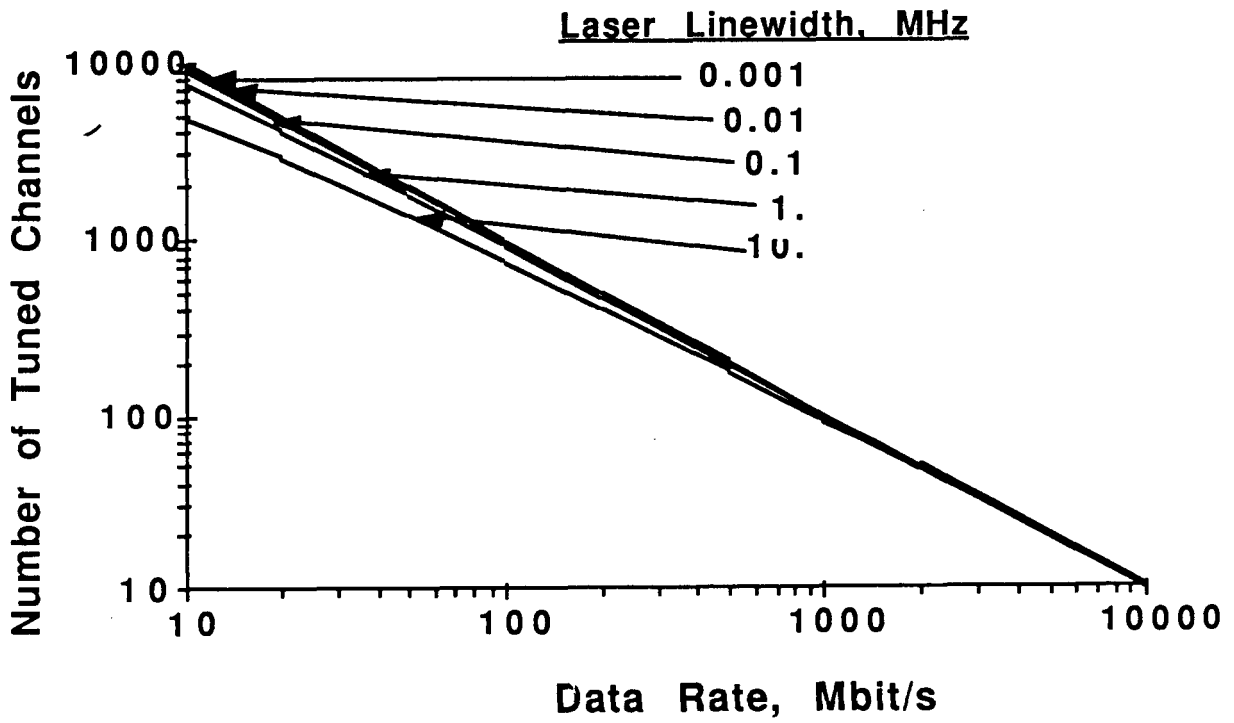

Figure 5. Digital System Channel Capacity.

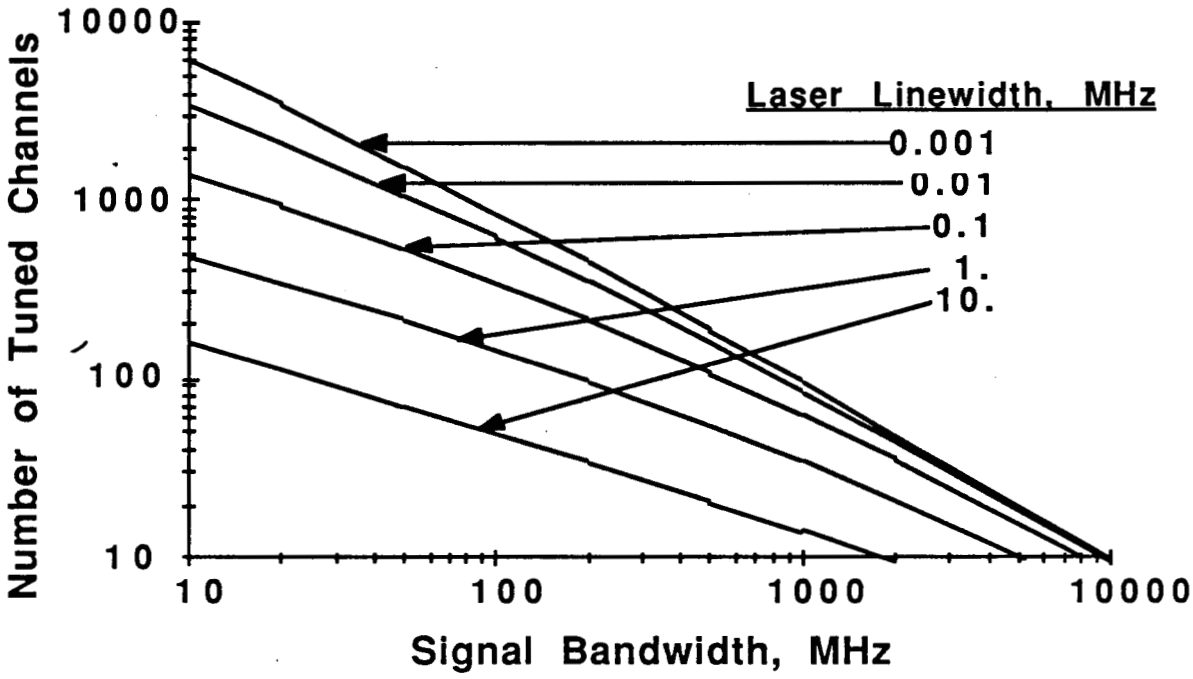

Figure 6. Analog Video System Channel Capacity.

With digital transmission the laser linewidth plays little role in determining system channel capacity, except at very low data rates. The laser tuning range sets a limit of approximately 100 channels at 1 Gbit/s and 10,000 channels at 10 Mbit/s. For the latter case, the linewidth must be narrower that 1 MHz or there will be a reduction in system channel capacity due to laser phase noise from adjacent channels.

Analog video system channel capacity depends strongly on laser linewidth, as seen in Figure 6. In order to achieve a system capacity of 1000 channels (10 MHz bandwidth, 60 dB CNR), the laser linewidth must be less that 100 kHz. A linewidth of 10 MHz, characteristic of current but now state-of-the-art DFB lasers would support only 200 channels.

System Capabilities of Present Device Technology

We have combined our review of laser diode optical characteristics with the analysis of multichannel coherent system requirements to determine the system capabilities of current and anticipated laser devices. Figure 7 shows a map of both device characteristics and system requirements on a plane of laser tuning range and laser linewidth. The white ovals represent the applications previously discussed. The digital applications, 100 and 1000 channels of 1 Gbit/s data, are essentially independent of linewidth, but their system channel capacity depends on the laser tuning range. The video application, 1000 channels at 10 MHz analog bandwidth, depends on both the linewidth and the tuning range.

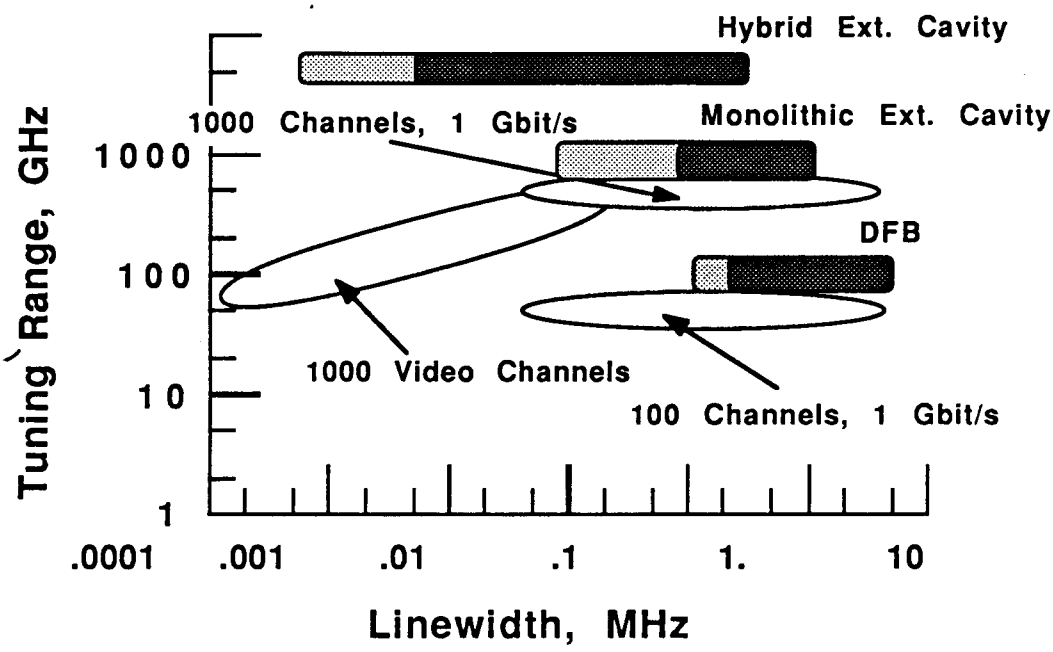

Figure 7. Coherent system applications and diode laser capabilities.

The shaded rectangles represent the capabilities of various device technologies. Dark shading indicates current capabilities, while light shading gives our estimate of the practical limits of future capabilities.

We see that the digital applications are within the capabilities of currently demonstrated monolithic technology. DFB lasers can accommodate 100 channels and monolithic external cavity devices can handle 1000 channels. Improvements in linewidth may not increase system channel capacity, but could improve link performance by allowing the use of modulation techniques with greater receiver sensitivity.

The video application is marginally achievable through the use of monolithic external cavity devices. This application requires both narrow linewidth and wide tuning range. Of course, reducing the number of channels would ease the requirements on both of these parameters.

Conclusions

We have reviewed the role of diode laser optical characteristics in determining the performance capabilities of coherent optical communication systems. Laser linewidth, wavelength tuning range, and wavelength stabilization are the key optical characteristics whose values impact the performance of all types of systems.

Laser diode technology now demonstrated in the laboratory has attained wavelength tuning range in excess of 500 GHz. This is adequate for the broadband multichannel applications discussed here. Wavelength stabilization performance needed for these applications has also been achieved using electronic tuning. Phase noise linewidths of 1 MHz are adequate for high

frequency digital systems, but are too great for analog systems requiring large carrier-to-noise ratios.

Overall, we see that the current laboratory performance of diode lasers for optical communications already meets the needs of advanced communications systems that use coherent techniques to achieve capacities vastly greater than present direct detection systems. While further performance records will undoubtedly be set, the pace of system development will be determined by progress in monolithic integration, performance reproducibility, and other system integration issues rather than absolute performance.

In closing, we emphasize that the actual usefulness of the types of systems used here for our analysis will depend primarily on economic factors. Alternate approaches based upon digital multiplexing and switching involve very different system architectures. All broadband fiber optic technologies are developing rapidly, but coherent techniques are the newest and thus furthest from maturity. Though this makes their widespread use more speculative, it also implies greater potential for development and the discovery of unrecognized capabilities.

This work was supported in part by NASA Langley Research Center.

References

1. C. H. Henry, "Theory of the Linewidth of Semiconductor Lasers," IEEE J. Quantum Electron. vol. QE-18, pp.259-285, 1982.

2. S. Murata, I. Mito, and K. Kobayashi, "Tuning Ranges for 1.5 μm Wavelength Tunable DBR Lasers," Electron. Lett. vol. 24, pp. 577-578,1988.

3. Y. Kotaki, M. Matsuda, H. Ishitawa, and H. Imai, "Tunable DBR Lasers with Wide Tuning Range," Electron Lett. Vol 24, pp 503-504, 1988.

4. J. Salz, "Coherent Lightwave Communications," AT&T Technical Journal, vol. 64, pp 2153-2209, December, 1985.

5. David W. Smith, "Techniques for Multigigibit Coherent Optical Transmission," IEEE J. Lightwave Tech. vol LT-5, pp 1466-1478, Oct. 1987.

6. Kigoshi Noso and Katsushi Iwashita, "A Consideration of Factors Affecting Future Coherent Lightwave Communication Systems," J. Lightwave Tech. vol LT-6, pp 686-694, May 1988.

7. Gerard J. Foschini, "Sharing of the Optical Band in Local Systems," IEEE J. on Selected Areas in Comm., vol SAC-6, pp 974-986, July, 1988.

8. Leonid G. Kazovsky, "Multichannel Coherent Optical Communications Systems," IEEE J. Lightwave Tech., vol LT-5, pp 1095-1102, August 1987.

9. Y. H. Cheng and T. Okoshi, "Effect of Laser Linewidth on Crosstalk Penelty in Two-Channel ASK Heterodyne Detection System," Electron. Lett., vol 24, pp 830-831, July, 1988.

NASA
National Aeronautics and Space Administration

Report Documentation Page

1. Report No.	2. Government Accession No.	3. Recipient's Catalog No.
NASA CR-181870		

4. Title and Subtitle
Monolithic Narrow Linewidth InGaAsP Semiconductor Laser for Coherent Optical Communications

5. Report Date
September 1989

6. Performing Organization Code

7. Author(s)
S. L. Palfrey, R. E. Enstrom, P. A. Longeway

8. Performing Organization Report No.

10. Work Unit No.
506-44-21

9. Performing Organization Name and Address
David Sarnoff Research Center
Princeton, NJ 08543-5300

11. Contract or Grant No.
NAS1-18539

13. Type of Report and Period Covered
Final Report
8/6/87 - 6/9/89

12. Sponsoring Agency Name and Address
National Aeronautics & Space Administration
Langley Research Center
Hampton, VA 23665-5225

14. Sponsoring Agency Code

15. Supplementary Notes
NASA-Langley Technical Monitor: H. D. Hendricks
Final Report - 8/6/87 - 6/9/89

16. Abstract

A design for a monolithic narrow-linewidth InGaAsP diode laser has been developed using a multiple-quantum-well (MQW) extended-passive-cavity distributed-Bragg-reflector (DBR) laser design. Theoretical results indicate that this structure has the potential for a linewidth of 100 kHz or less. To realize this device, a number of the fabrication techniques required to integrate low-loss passive waveguides with active regions have been developed using a DBR laser structure. In addition, the MOCVD growth of InGaAs MQW laser structures has been developed, and threshold current densities as low as 1.6 kA/cm^2 have been obtained from broad-stripe InGaAs/InGaAsP separate-confinement-heterostructure MQW lasers.

17. Key Words (Suggested by Author(s))	18. Distribution Statement
InGaAsP diode laser; laser linewidth; multiple-quantum-well laser; distributed-Bragg-reflector laser; coherent optical communications	Unclassified - Unlimited Subject Category 36

19. Security Classif. (of this report)	20. Security Classif. (of this page)	21. No. of pages	22. Price
Unclassified	Unclassified	58	

NASA FORM 1626 OCT 86